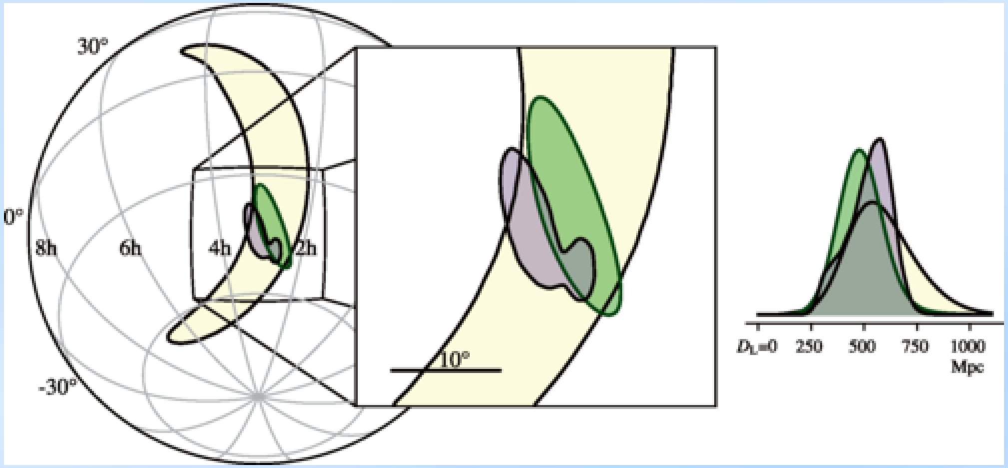

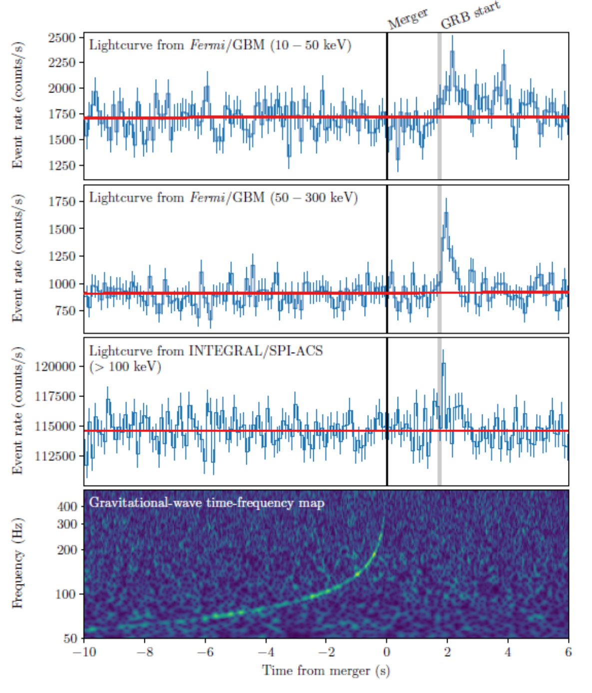

Gravitational Waves: Past, Present and Future

Nelson Christensen, Artemis

Observatoire de la Côte d’Azur, Nice

November 22, 2021 LPNHE

General Relativity

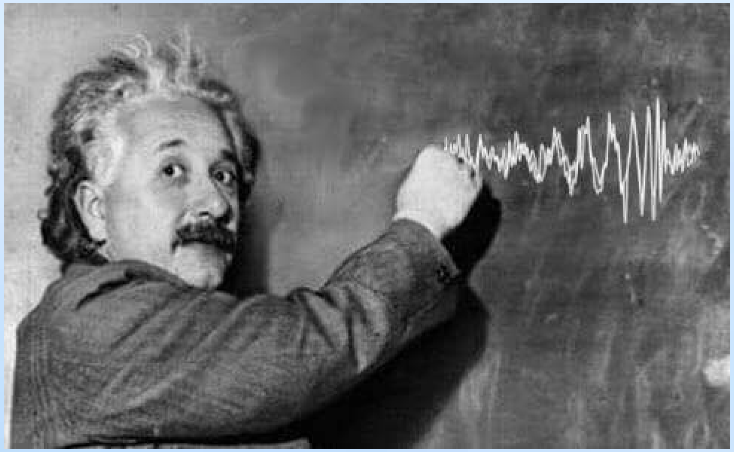

1915: Einstein’s Theory of General Relativity

1916: Einstein paper on linear approximation to general relativity with multiple applications, including gravitational waves.

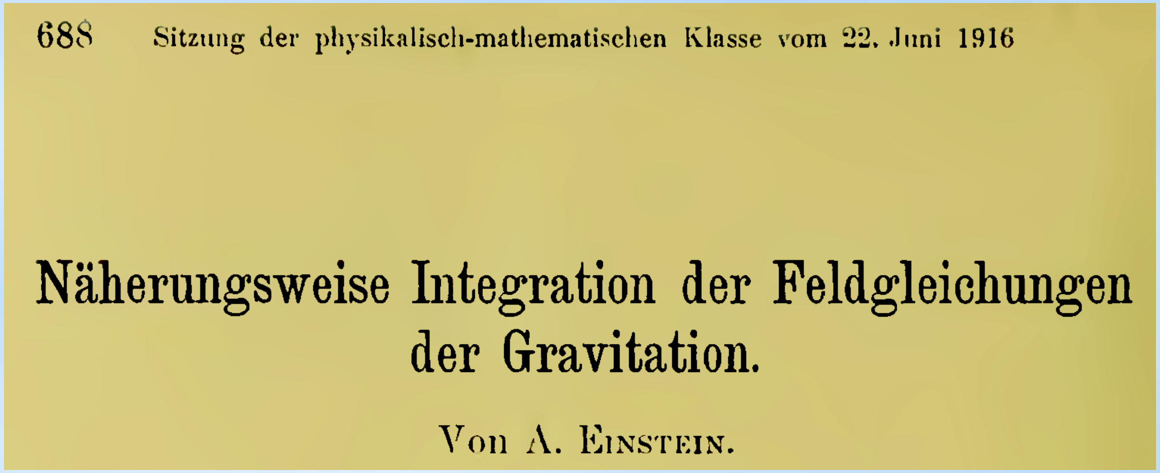

688 Sitzung der physikalisch-mathematischen Klasse vom 22. Juni 1916

Näherungsweise Integration der Feldgleichungen der Gravitation.

Von A. Einstein.

Approximative Integration of the Field Equations of Gravitation

Gravitational Waves

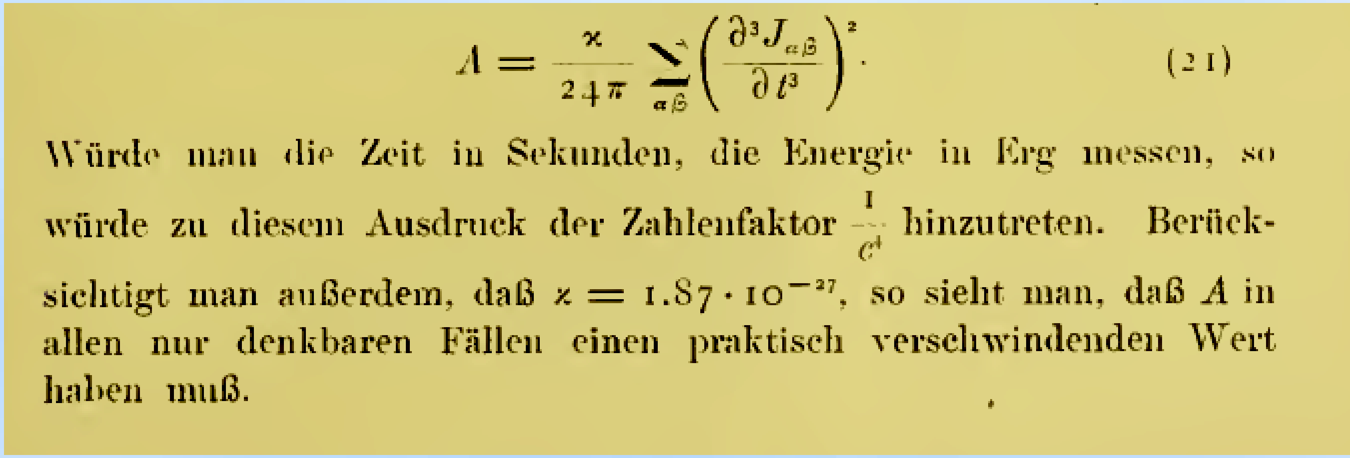

$$A = \frac{\varkappa}{24\pi} \sum_{\alpha\beta} \left(\frac{\partial^3 J_{\alpha\beta}}{\partial t^3} \right)^2 . \qquad (21)$$

Würde man die Zeit in Sekunden, die Energie in Erg messen, so würde zu diesem Ausdruck der Zahlenfaktor $\frac{1}{c^4}$ hinzutreten. Berücksichtigt man außerdem, daß $\varkappa = 1.87 \cdot 10^{-27}$, so sieht man, daß A in allen nur denkbaren Fällen einen praktisch verschwindenden Wert haben muß.

"… in all conceivable cases, ***A*** must have a practically vanishing value."

Gravitational waves are predicted by Einstein, but he recognizes that they are too small.

Gravitational Waves

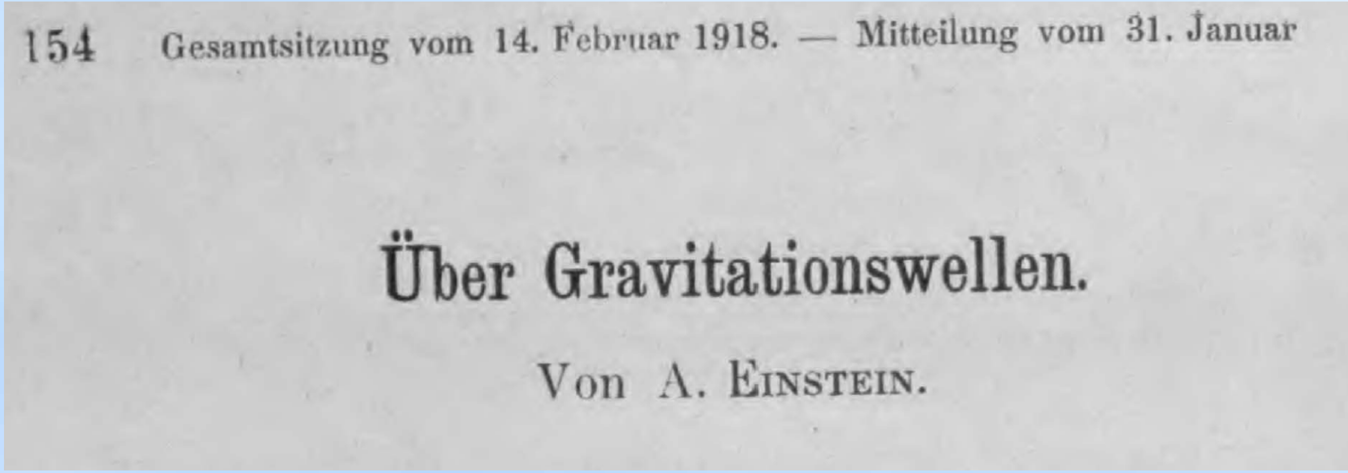

154 Gesamtsitzung vom 14. Februar 1918. — Mitteilung vom 31. Januar

Über Gravitationswellen.

Von A. Einstein.

On Gravitational Waves – 1918

Einstein works out the remaining details on gravitational waves: emission (quadrupole), polarizations, they carry energy, etc

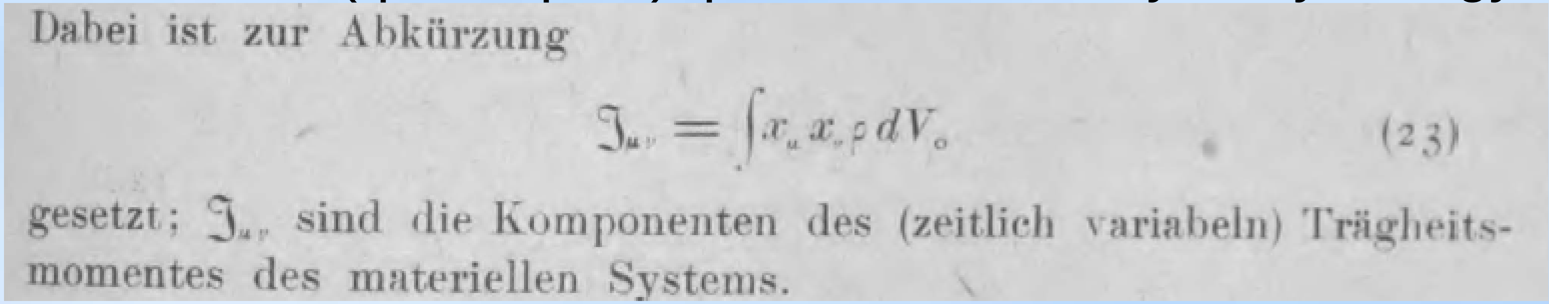

Dabei ist zur Abkürzung

$$\mathfrak{J}_{\mu\nu} = \int x_\mu x_\nu \rho \, dV_0 \qquad (23)$$

gesetzt; $\mathfrak{J}_{\mu\nu}$ sind die Komponenten des (zeitlich variabeln) Trägheitsmomentes des materiellen Systems.

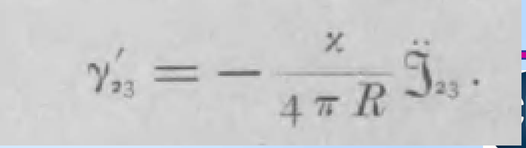

$$\gamma'_{23} = -\frac{\varkappa}{4\pi R}\ddot{\mathfrak{J}}_{23} .$$

While we are at it … Black Holes!

Über das Gravitationsfeld eines Massenpunktes nach der Einsteinschen Theorie.

Von K. Schwarzschild.

(Vorgelegt am 13. Januar 1916 [s. oben S. 42].)

On the gravitational field of a mass point according to Einstein's theory

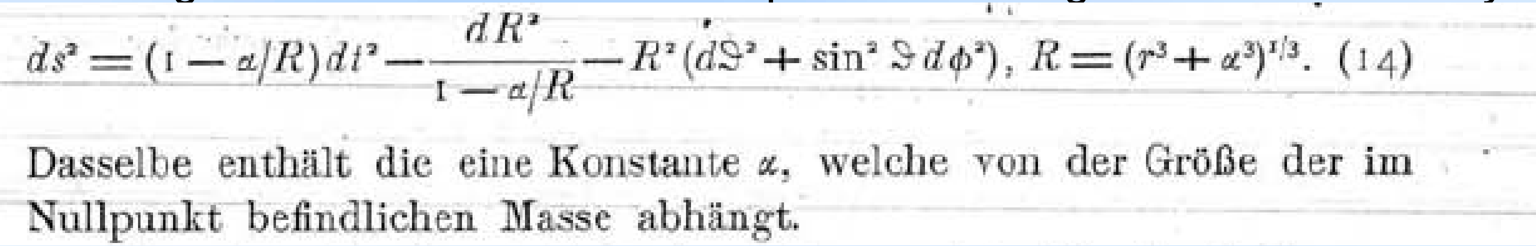

$$ds^2 = (1-\alpha/R)\,dt^2 - \frac{dR^2}{1-\alpha/R} - R^2(d\vartheta^2 + \sin^2\vartheta\, d\phi^2), \quad R = (r^3+\alpha^3)^{1/3}. \quad (14)$$

Dasselbe enthält die eine Konstante α, welche von der Größe der im Nullpunkt befindlichen Masse abhängt.

The concept of a “Black Hole” was not recognized by Schwarschild:
A. Eddington 1924, G. Lemaître 1933, R. Oppenheimer 1939, D. Finkelstein 1958, …

Are Gravitational Waves Real?

Continued debate on whether gravitational waves really exist up until 1957 Chapel Hill conference.

Felix Pirani paper and presentation: relative acceleration of particle pairs can be associated with the Riemann tensor. The interpretation of the attendees was that non-zero components of the Riemann tensor were due to gravitational waves.

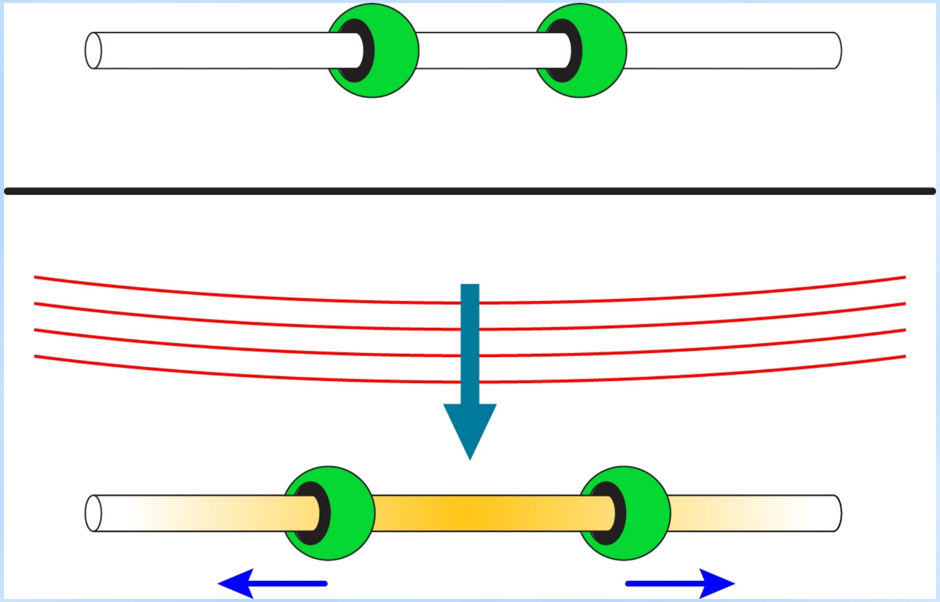

Sticky bead (Felix Pirani, Richard Feynman, Hermann Bondi)

Joe Weber of the University of Maryland, and from this inspiration started to think about gravitational wave detection.

Binary Pulsar PSR 1913+16

M1 = 1.438 M_o

M2 = 1.390 M_o

8 hour orbit

Orbit decays by 3mm per orbit.

Discovered in 1974 by Russell Hulse and Joseph Taylor, then at University Massachusetts.

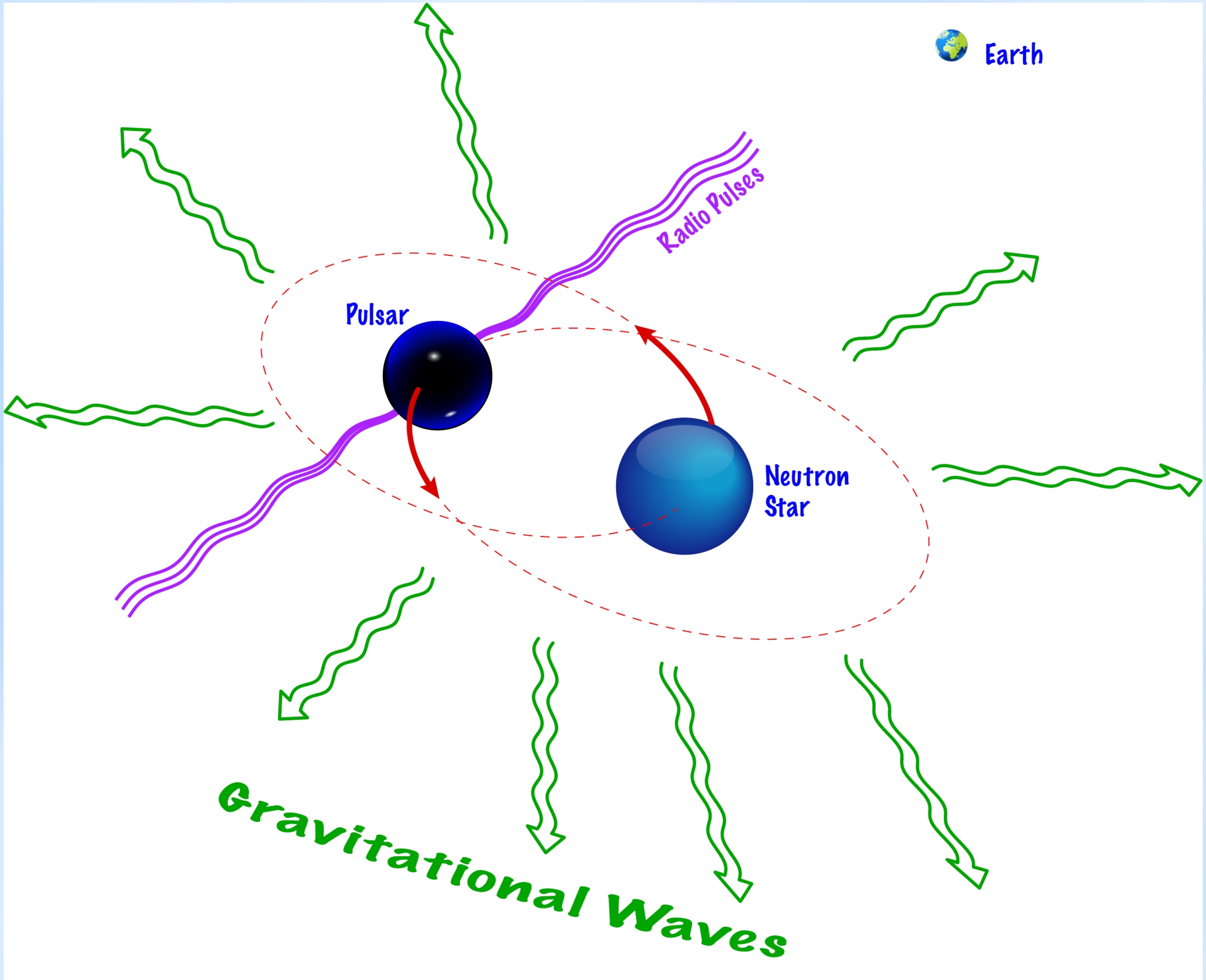

First Proof That Gravitational Waves Exist - 1982

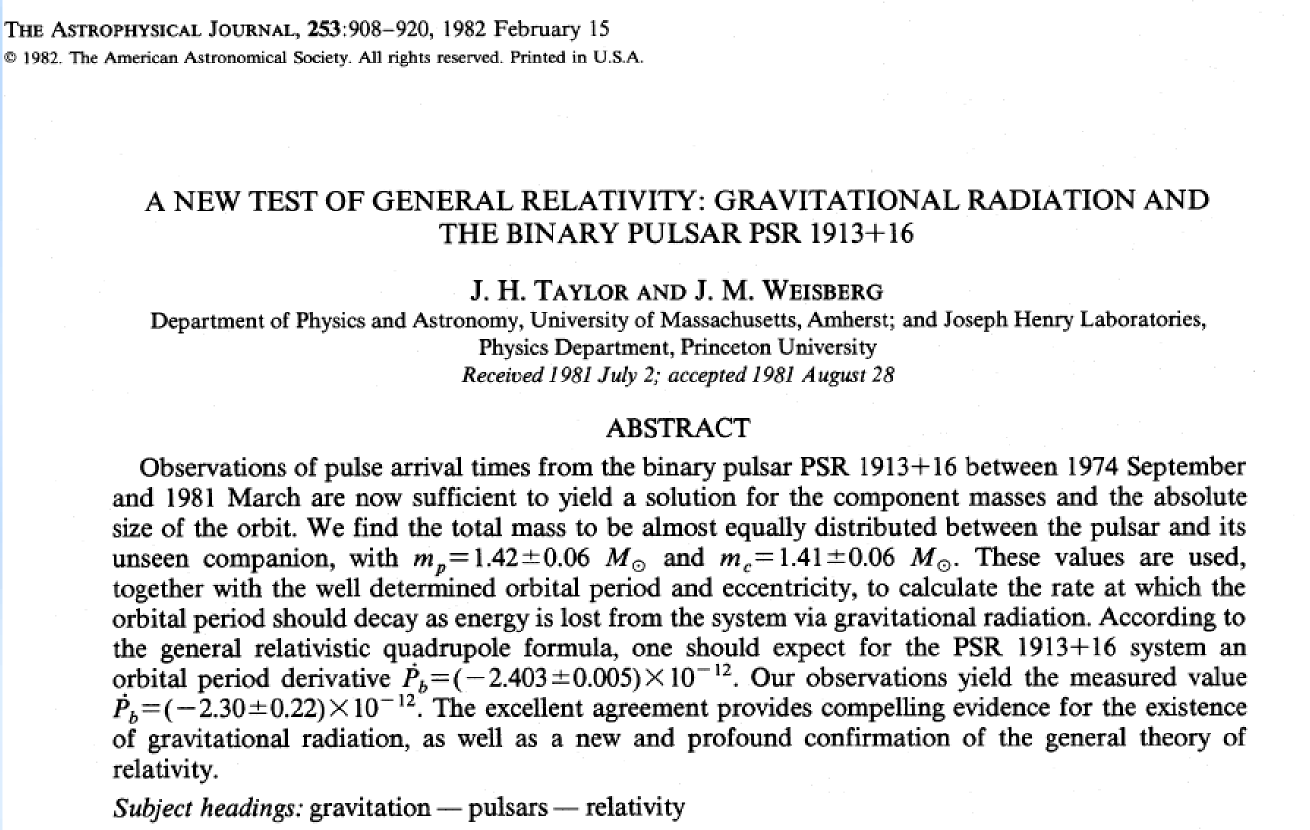

THE ASTROPHYSICAL JOURNAL, **253**:908–920, 1982 February 15

A NEW TEST OF GENERAL RELATIVITY: GRAVITATIONAL RADIATION AND THE BINARY PULSAR PSR 1913+16

J. H. TAYLOR AND J. M. WEISBERG
Department of Physics and Astronomy, University of Massachusetts, Amherst; and Joseph Henry Laboratories,
Physics Department, Princeton University

Received 1981 July 2; accepted 1981 August 28

ABSTRACT

Observations of pulse arrival times from the binary pulsar PSR 1913+16 between 1974 September and 1981 March are now sufficient to yield a solution for the component masses and the absolute size of the orbit. We find the total mass to be almost equally distributed between the pulsar and its unseen companion, with $m_p = 1.42 \pm 0.06\ M_\odot$ and $m_c = 1.41 \pm 0.06\ M_\odot$. These values are used, together with the well determined orbital period and eccentricity, to calculate the rate at which the orbital period should decay as energy is lost from the system via gravitational radiation. According to the general relativistic quadrupole formula, one should expect for the PSR 1913+16 system an orbital period derivative $\dot{P}_b = (-2.403 \pm 0.005) \times 10^{-12}$. Our observations yield the measured value $\dot{P}_b = (-2.30 \pm 0.22) \times 10^{-12}$. The excellent agreement provides compelling evidence for the existence of gravitational radiation, as well as a new and profound confirmation of the general theory of relativity.

Subject headings: gravitation — pulsars — relativity

Gravitational Wave Proof

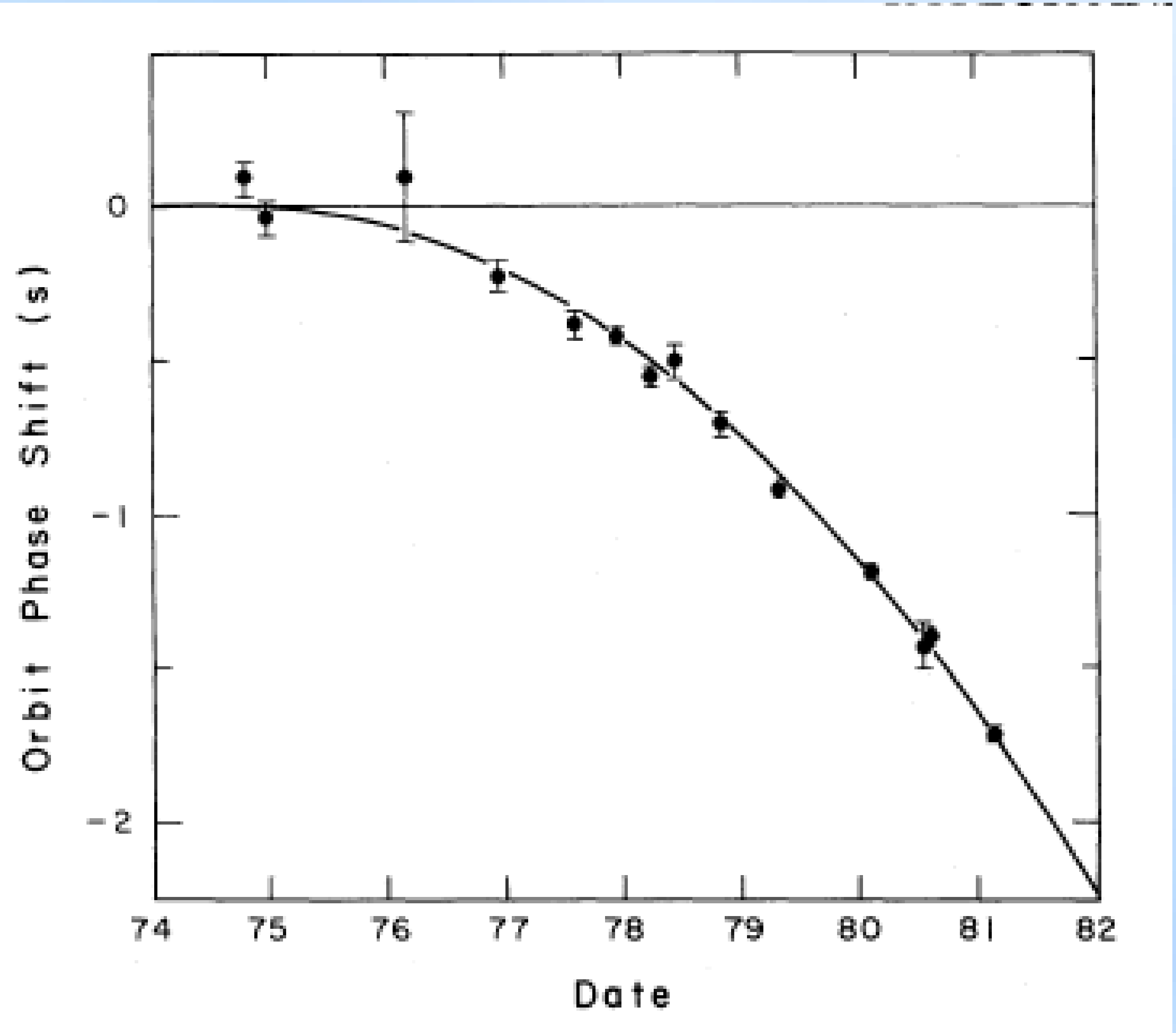

Taylor and Weisberg, 1982

Binary Pulsar Studies Continue

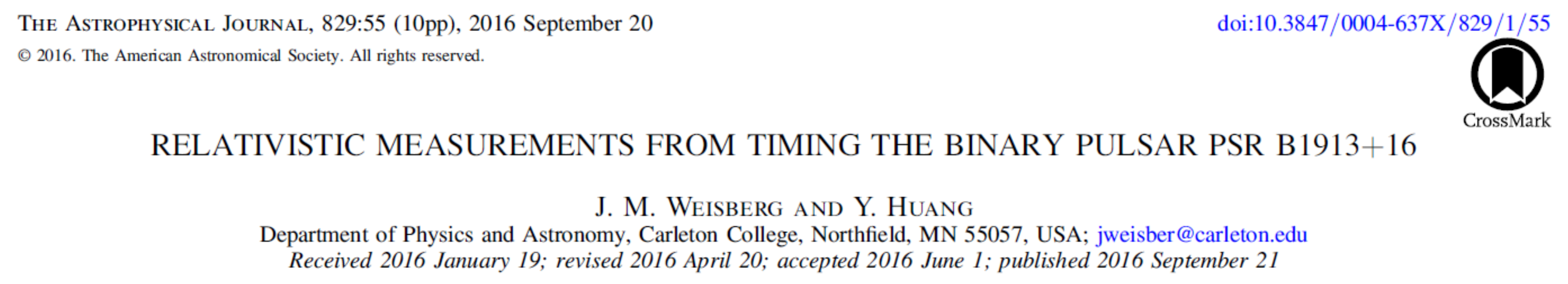

The Astrophysical Journal, 829:55 (10pp), 2016 September 20

doi:10.3847/0004-637X/829/1/55

CrossMark

RELATIVISTIC MEASUREMENTS FROM TIMING THE BINARY PULSAR PSR B1913+16

J. M. Weisberg and Y. Huang
Department of Physics and Astronomy, Carleton College, Northfield, MN 55057, USA; jweisber@carleton.edu

Received 2016 January 19; revised 2016 April 20; accepted 2016 June 1; published 2016 September 21

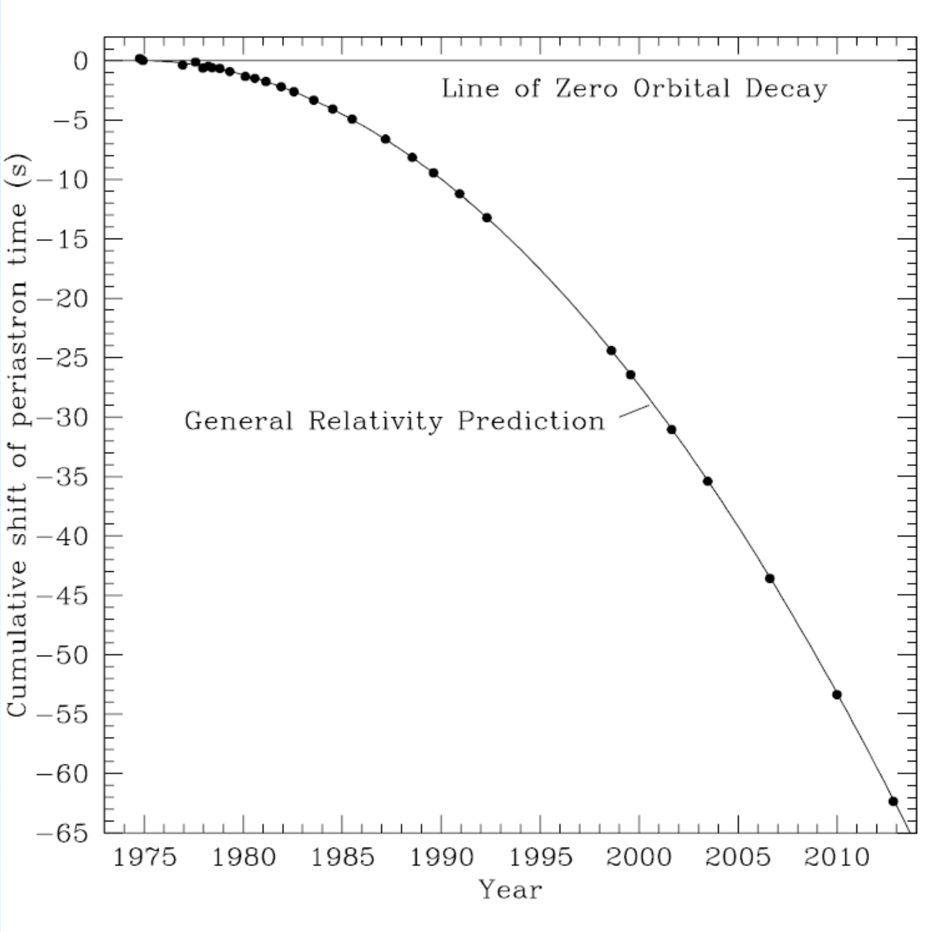

“The points, with error bars too small to show, represent our measurements”

Advanced LIGO – Advanced Virgo Network

LIGO Lab/Virgo

LIGO, Livingston,
Louisiana, USA
4 km

LIGO, Hanford,
Washington, USA
4 km

Virgo, Cascina,
Pisa, Italy
3 km

Three observing runs so far completed
O4 in late 2022, 12-18 months in duration
KAGRA (3 km, underground, cryogenic mirrors) in Japan will join

The Detectors

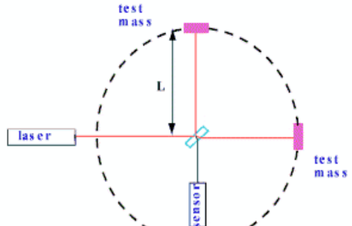

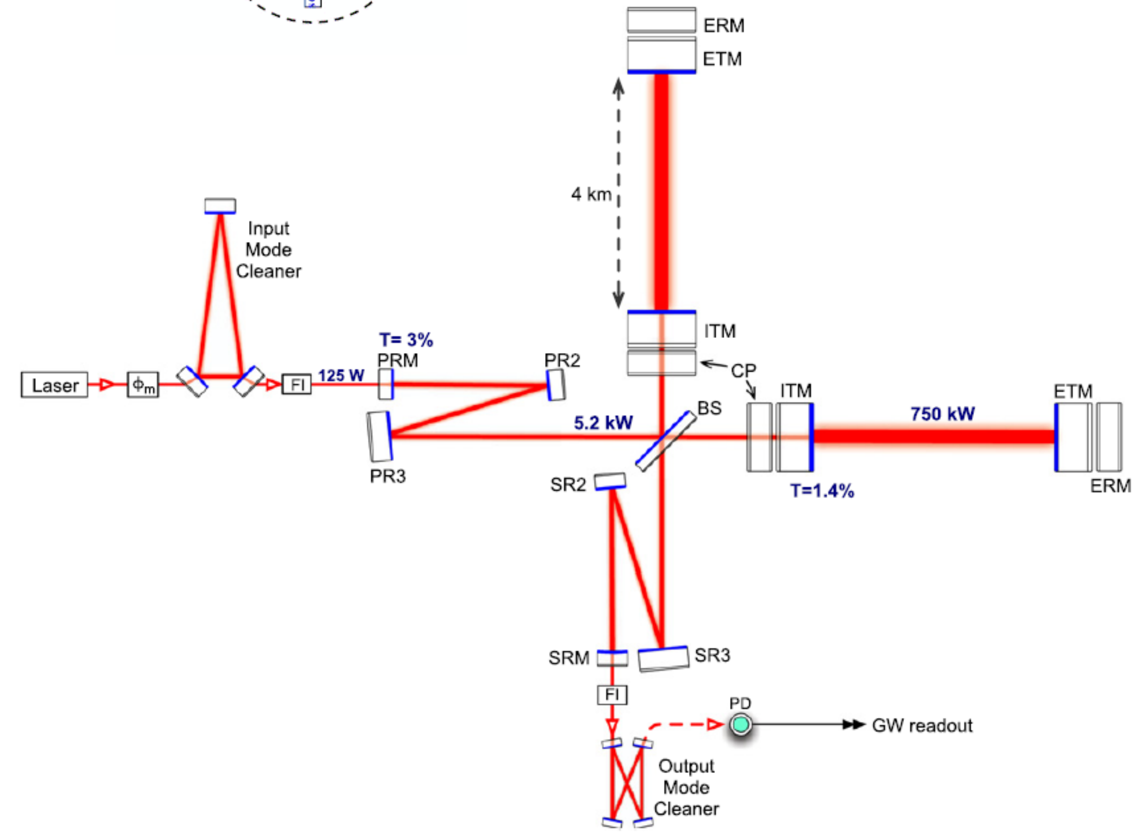

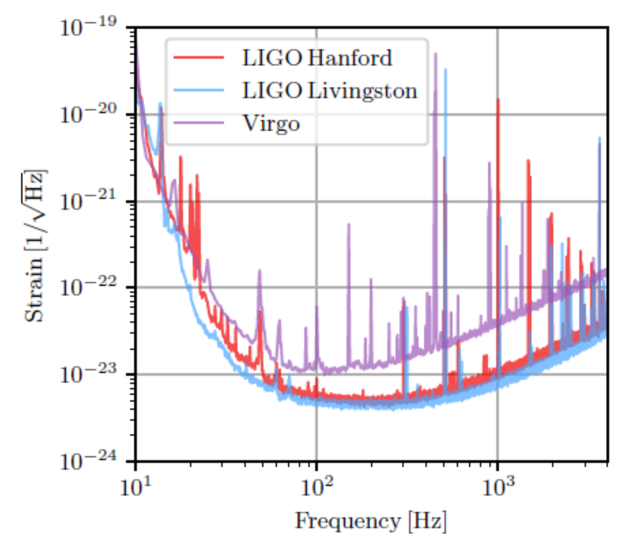

O3 sensitivities

Advanced LIGO Target Design
4 km arms

Advanced Virgo

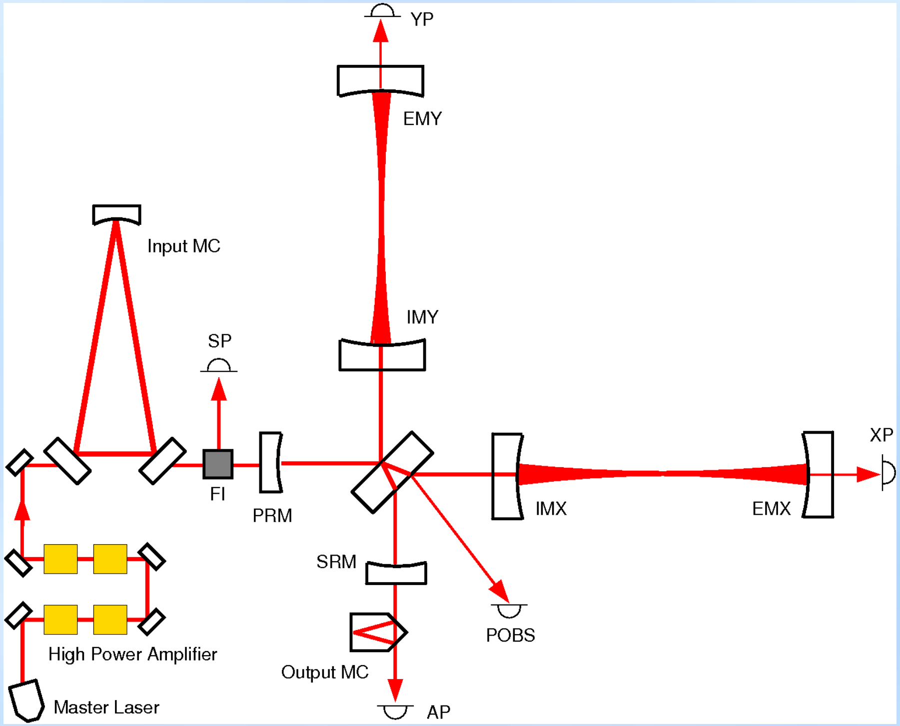

- Larger mirrors; better optical quality.
- Higher finesse of the arm cavities
- Increased laser power.
- Came on-line August 2017.

Advanced Virgo

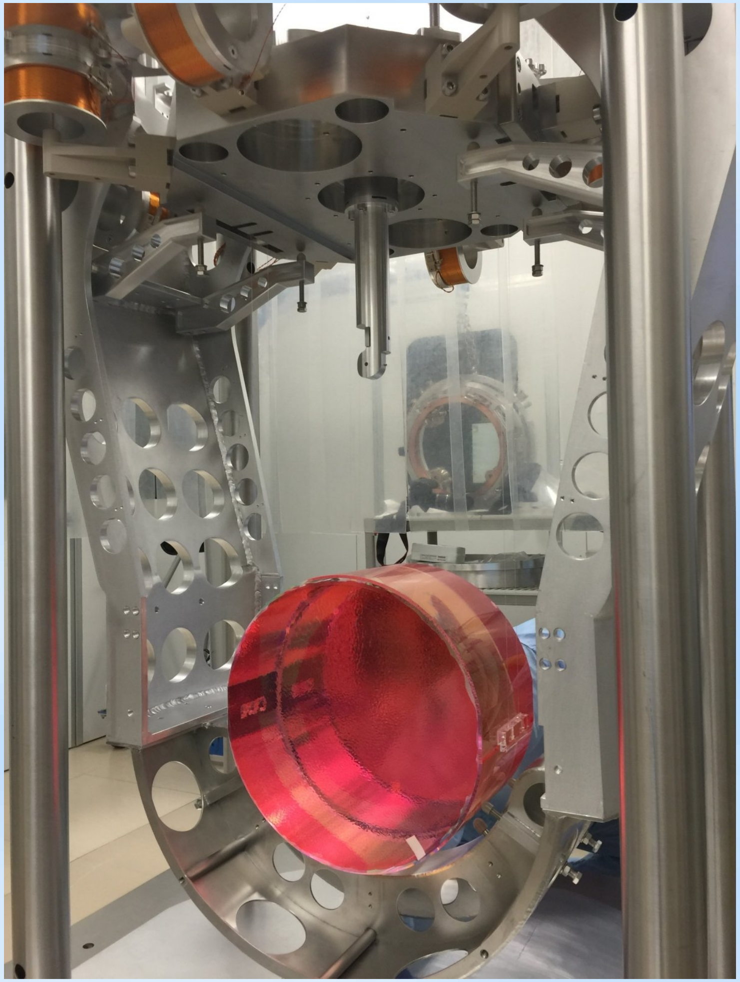

Mirror

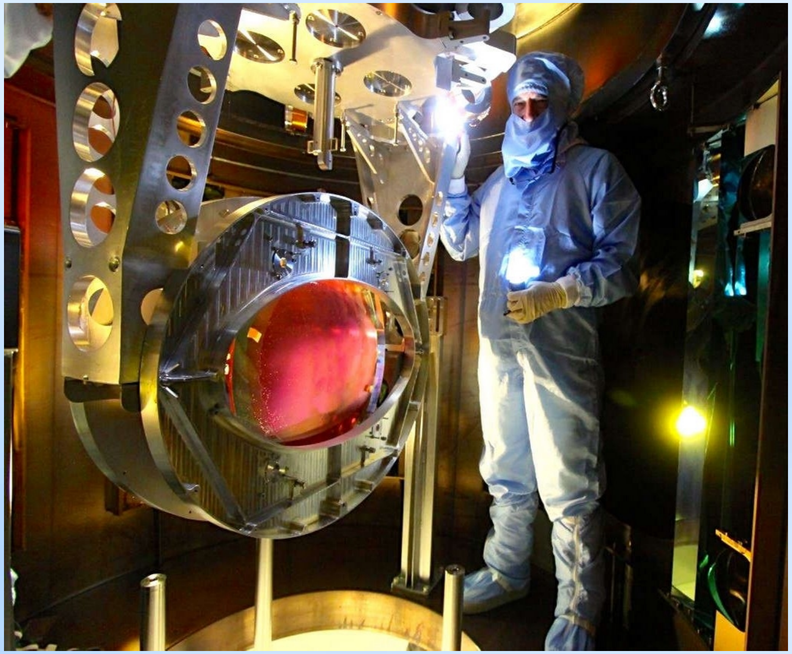

Beamsplitter

The optical components are very large, but their quality is exquisite.

O1 – GW150914 – First Discovery

- Band-pass filter:
  35-350 Hz
- L1-H1 time delay of about 7ms.
- Chirp signal, typical of binary coalescences.
- Detected by online burst-search pipelines.
- Confirmed later matched template searches.
- Combined SNR: 24.

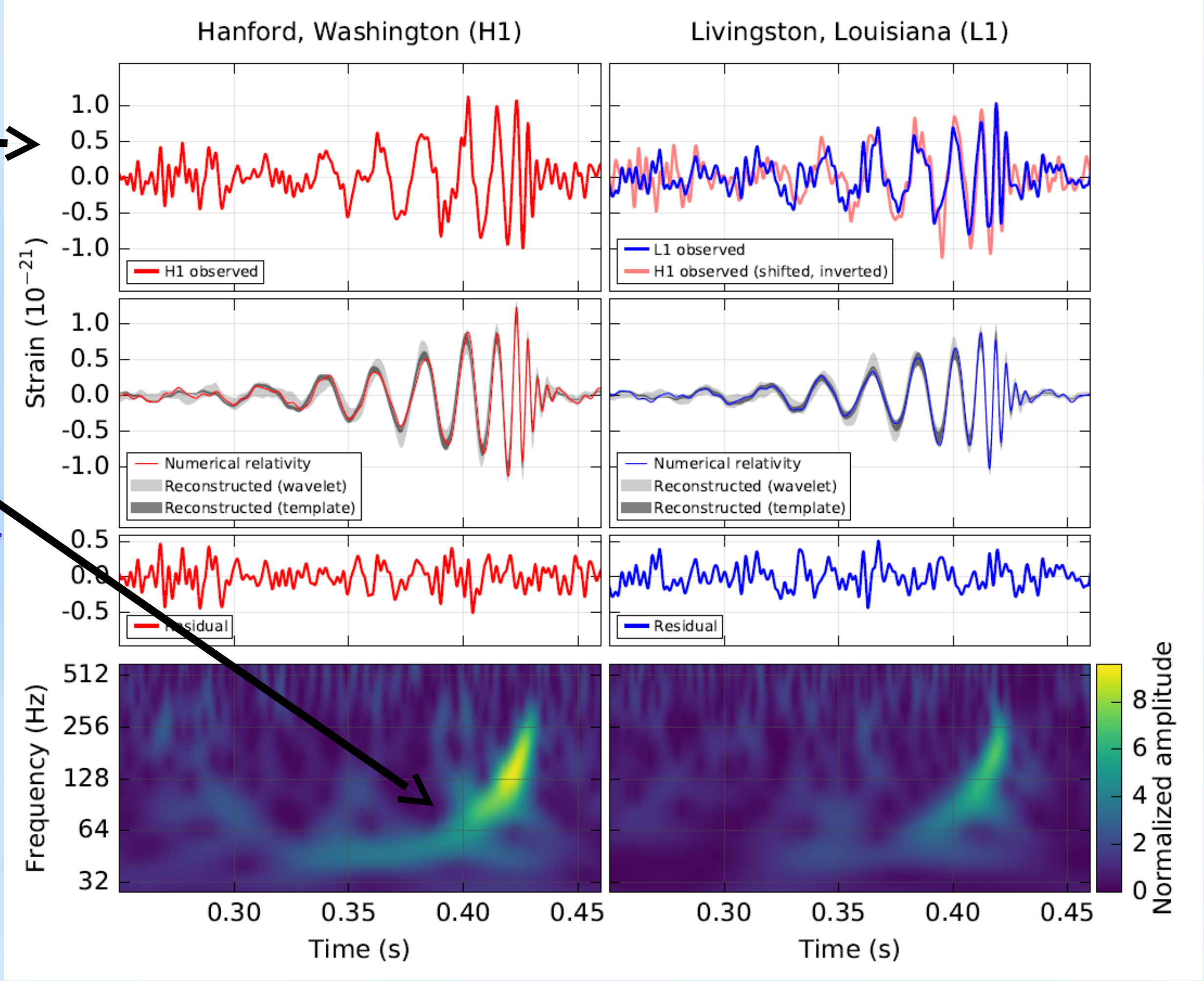

The Results

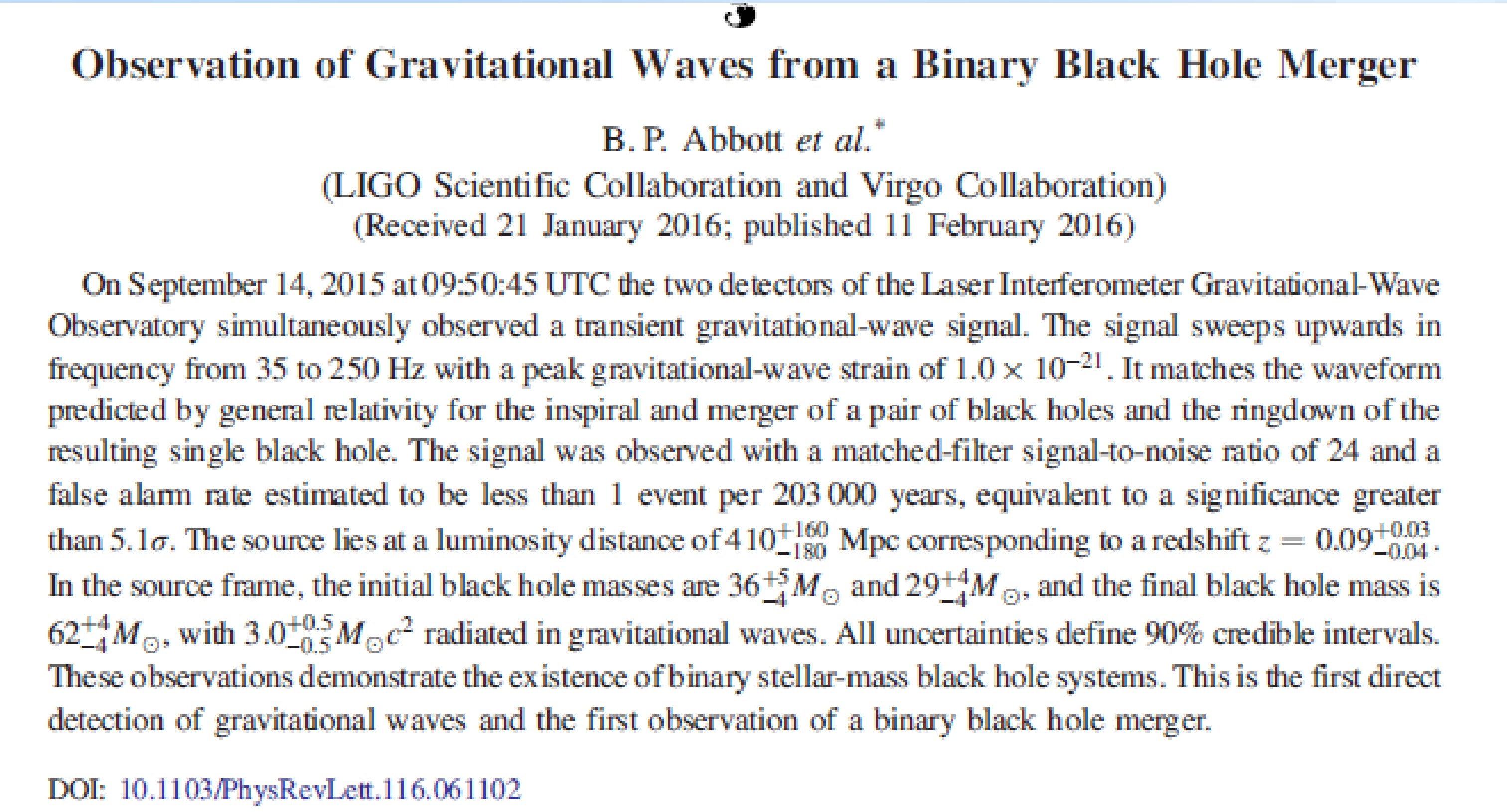

Observation of Gravitational Waves from a Binary Black Hole Merger

B. P. Abbott *et al.*[*]
(LIGO Scientific Collaboration and Virgo Collaboration)

(Received 21 January 2016; published 11 February 2016)

On September 14, 2015 at 09:50:45 UTC the two detectors of the Laser Interferometer Gravitational-Wave Observatory simultaneously observed a transient gravitational-wave signal. The signal sweeps upwards in frequency from 35 to 250 Hz with a peak gravitational-wave strain of 1.0×10^{-21}. It matches the waveform predicted by general relativity for the inspiral and merger of a pair of black holes and the ringdown of the resulting single black hole. The signal was observed with a matched-filter signal-to-noise ratio of 24 and a false alarm rate estimated to be less than 1 event per 203 000 years, equivalent to a significance greater than 5.1σ. The source lies at a luminosity distance of 410^{+160}_{-180} Mpc corresponding to a redshift $z = 0.09^{+0.03}_{-0.04}$. In the source frame, the initial black hole masses are $36^{+5}_{-4} M_\odot$ and $29^{+4}_{-4} M_\odot$, and the final black hole mass is $62^{+4}_{-4} M_\odot$, with $3.0^{+0.5}_{-0.5} M_\odot c^2$ radiated in gravitational waves. All uncertainties define 90% credible intervals. These observations demonstrate the existence of binary stellar-mass black hole systems. This is the first direct detection of gravitational waves and the first observation of a binary black hole merger.

DOI: 10.1103/PhysRevLett.116.061102

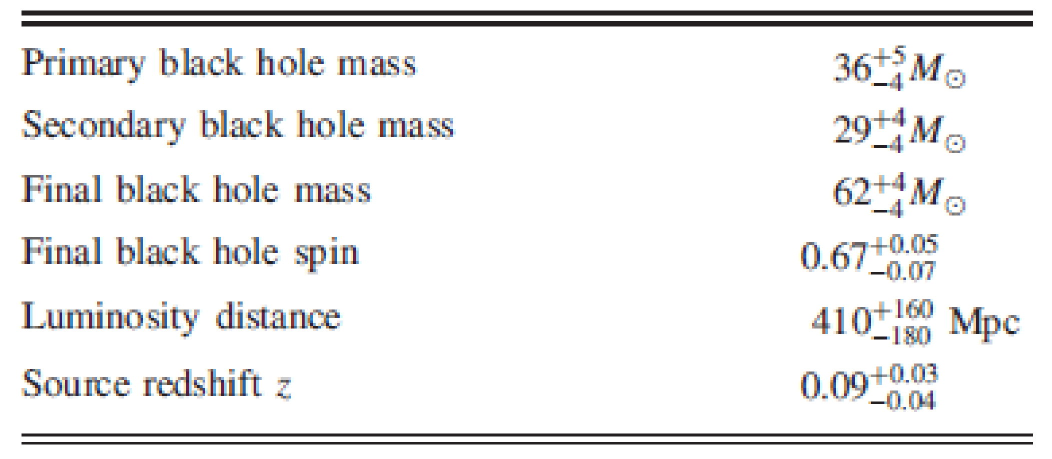

Primary black hole mass	$36^{+5}_{-4} M_\odot$
Secondary black hole mass	$29^{+4}_{-4} M_\odot$
Final black hole mass	$62^{+4}_{-4} M_\odot$
Final black hole spin	$0.67^{+0.05}_{-0.07}$
Luminosity distance	410^{+160}_{-180} Mpc
Source redshift z	$0.09^{+0.03}_{-0.04}$

GW170814 – 3 Detector Observation

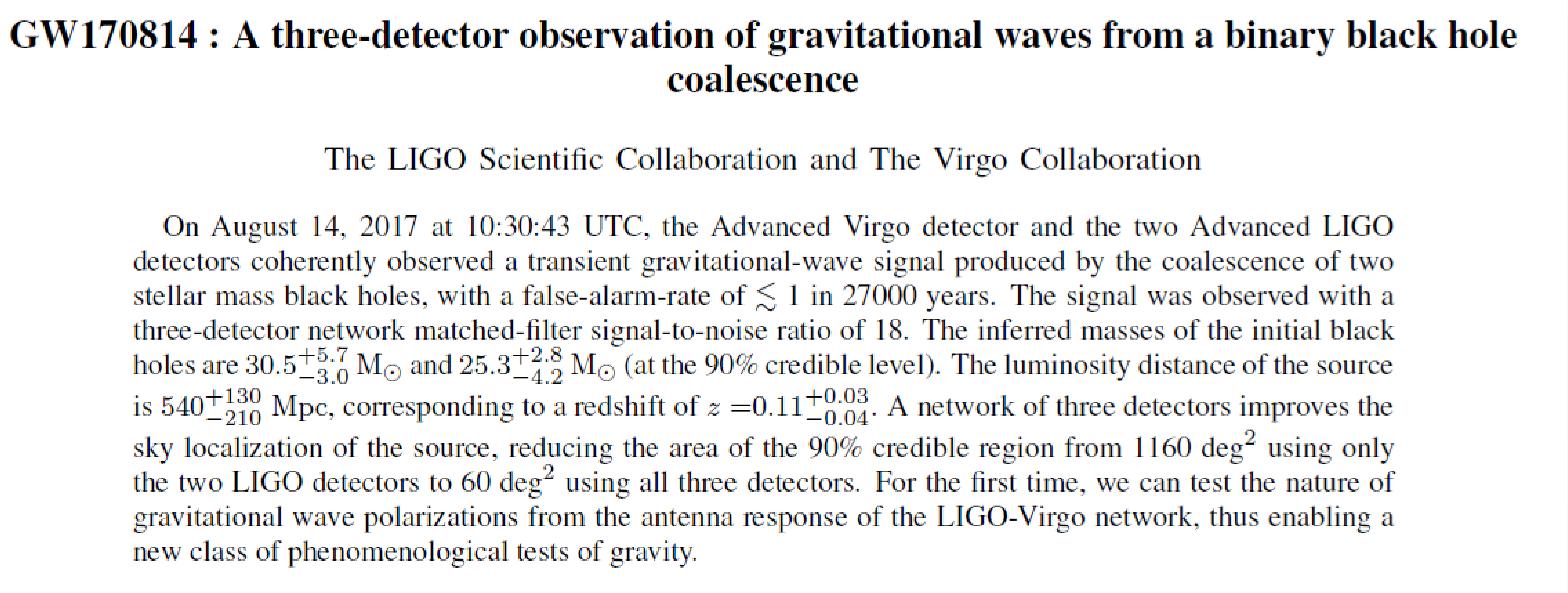

GW170814 : A three-detector observation of gravitational waves from a binary black hole coalescence

The LIGO Scientific Collaboration and The Virgo Collaboration

On August 14, 2017 at 10:30:43 UTC, the Advanced Virgo detector and the two Advanced LIGO detectors coherently observed a transient gravitational-wave signal produced by the coalescence of two stellar mass black holes, with a false-alarm-rate of $\lesssim 1$ in 27000 years. The signal was observed with a three-detector network matched-filter signal-to-noise ratio of 18. The inferred masses of the initial black holes are $30.5^{+5.7}_{-3.0}\,\mathrm{M}_\odot$ and $25.3^{+2.8}_{-4.2}\,\mathrm{M}_\odot$ (at the 90% credible level). The luminosity distance of the source is 540^{+130}_{-210} Mpc, corresponding to a redshift of $z = 0.11^{+0.03}_{-0.04}$. A network of three detectors improves the sky localization of the source, reducing the area of the 90% credible region from 1160 deg^2 using only the two LIGO detectors to 60 deg^2 using all three detectors. For the first time, we can test the nature of gravitational wave polarizations from the antenna response of the LIGO-Virgo network, thus enabling a new class of phenomenological tests of gravity.

Virgo has arrived!

A real world-wide network of gravitational wave detectors.

PRL

GW170814 – 3 Detector Observation

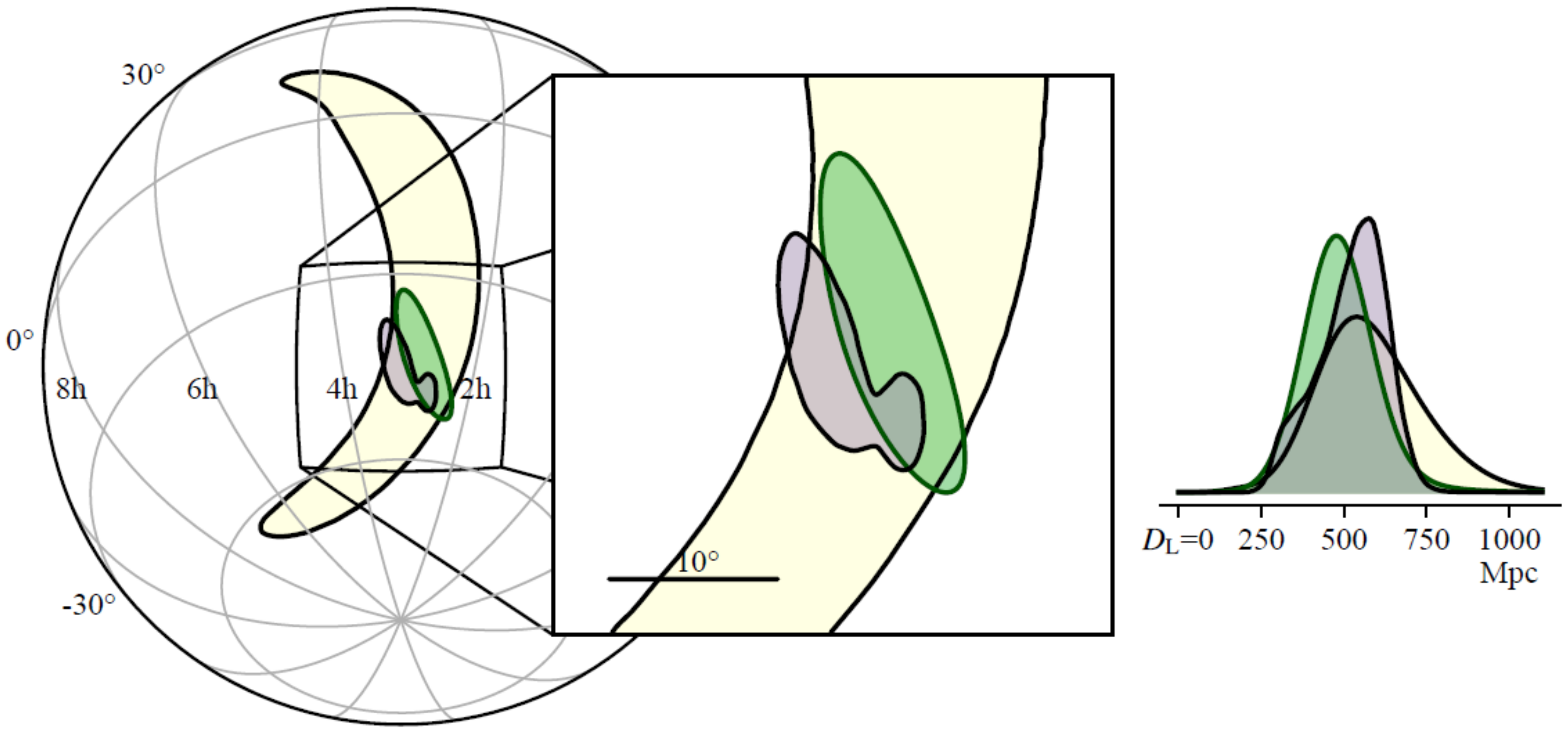

FIG. 3: Localization of GW170814. The rapid localization using data from the two LIGO sites is shown in yellow, with the inclusion of data from Virgo shown in green. The full Bayesian localization is shown in purple. The contours represent the 90% credible regions. The left panel is an orthographic projection and the inset in the center is a gnomonic projection; both are in equatorial coordinates. The inset on the right shows the posterior probability distribution for the luminosity distance, marginalized over the whole sky.

1160 sq. deg 2 LIGOs only → 60 sq. deg for 2 LIGOs + Virgo

Testing General Relativity With GW170814

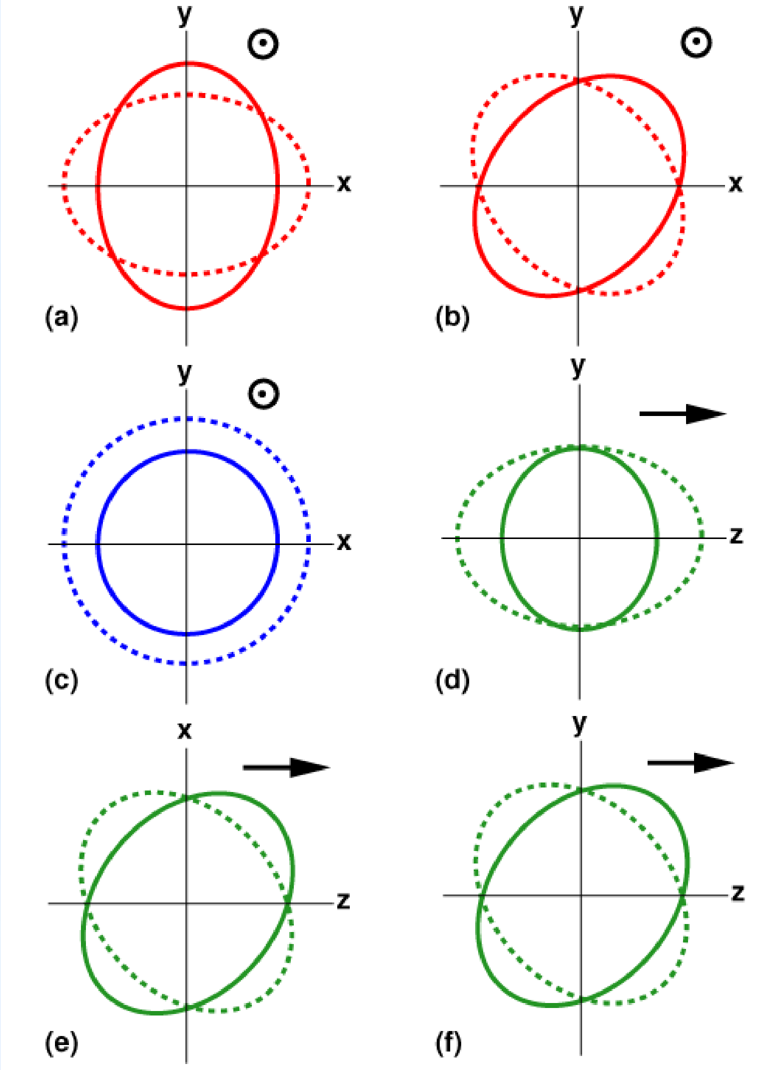

We now have a network of detectors with different orientations (2 LIGO are almost co-aligned, Virgo is not).

Allows the study of polarization of the gravitational waves.

Results favor purely tensor polarization against purely vector and purely scalar.

Tests of GR performed similar to those carried out for the previous confirmed detections — similar results, consistent with the predictions of Einstein's theory.

Post-Newtonian tests, signal consistency, ...

Clifford Will, Living Reviews in Relativity)

GW170817 – The Birth of GW Multi-Messenger Astronomy

17 August 2017

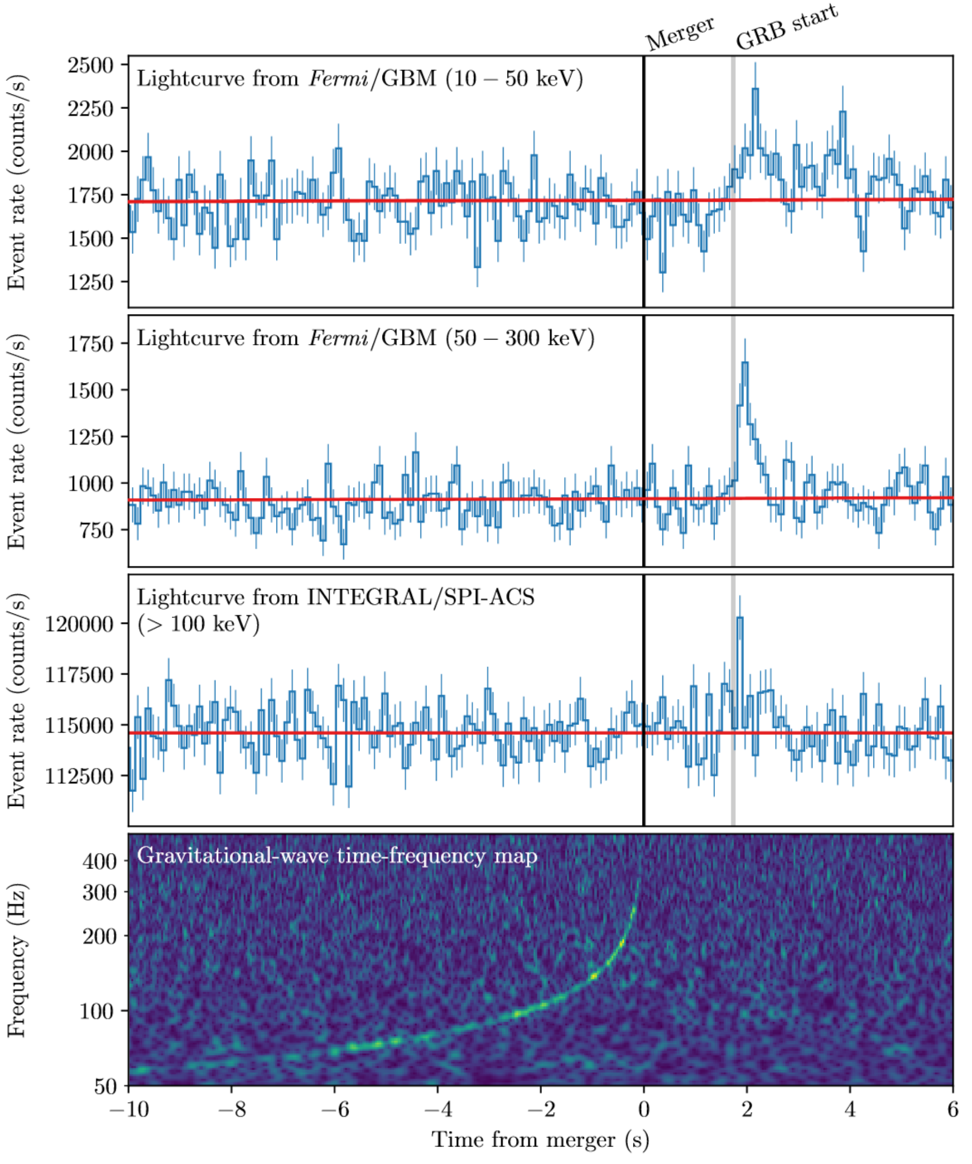

GW170817 – Host Galaxy Found

T_0 + 12 hours :
Alert sent from
1m2H Swope

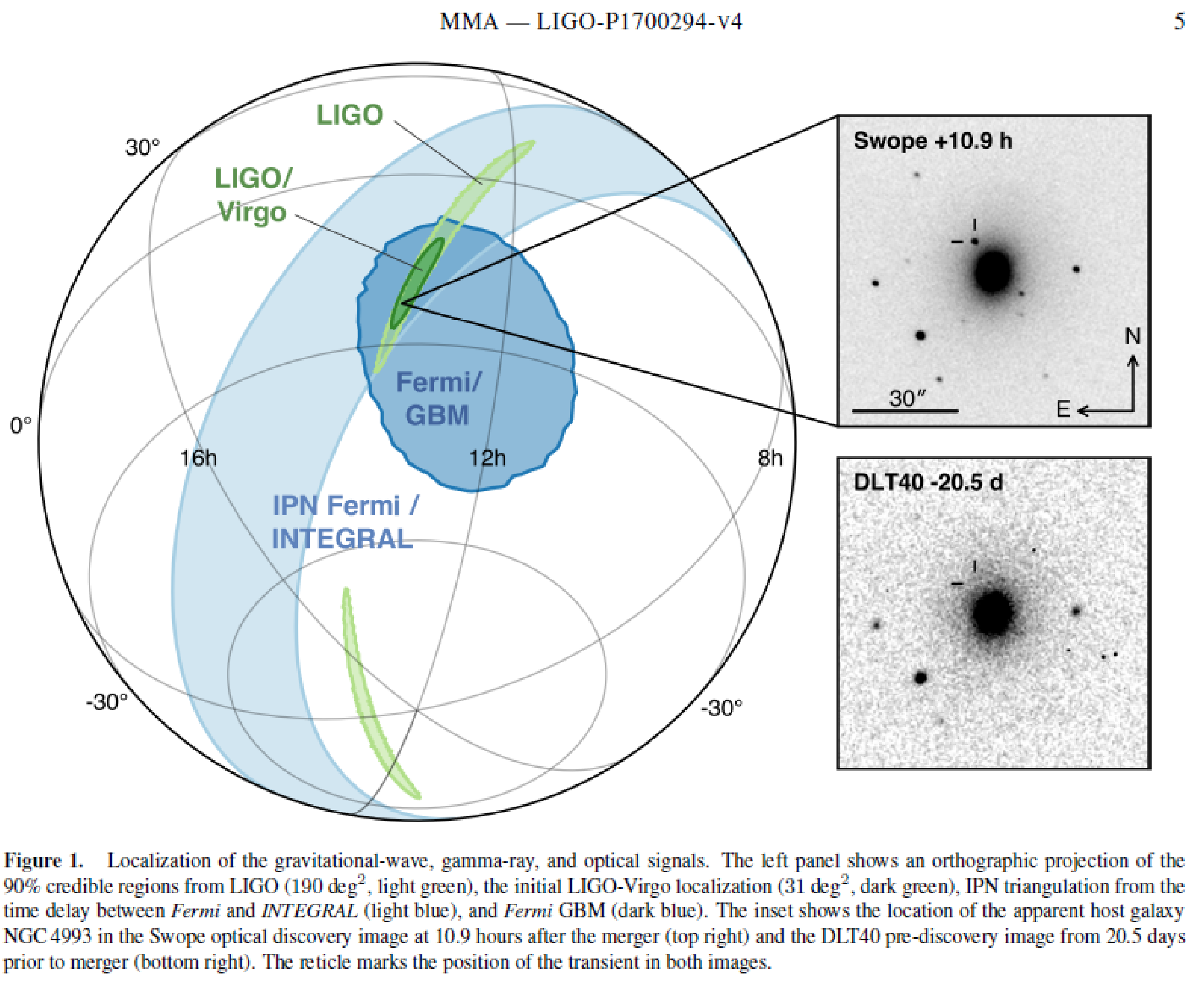

MMA — LIGO-P1700294-v4 5

Figure 1. Localization of the gravitational-wave, gamma-ray, and optical signals. The left panel shows an orthographic projection of the 90% credible regions from LIGO (190 deg^2, light green), the initial LIGO-Virgo localization (31 deg^2, dark green), IPN triangulation from the time delay between *Fermi* and *INTEGRAL* (light blue), and *Fermi* GBM (dark blue). The inset shows the location of the apparent host galaxy NGC 4993 in the Swope optical discovery image at 10.9 hours after the merger (top right) and the DLT40 pre-discovery image from 20.5 days prior to merger (bottom right). The reticle marks the position of the transient in both images.

Kilonova

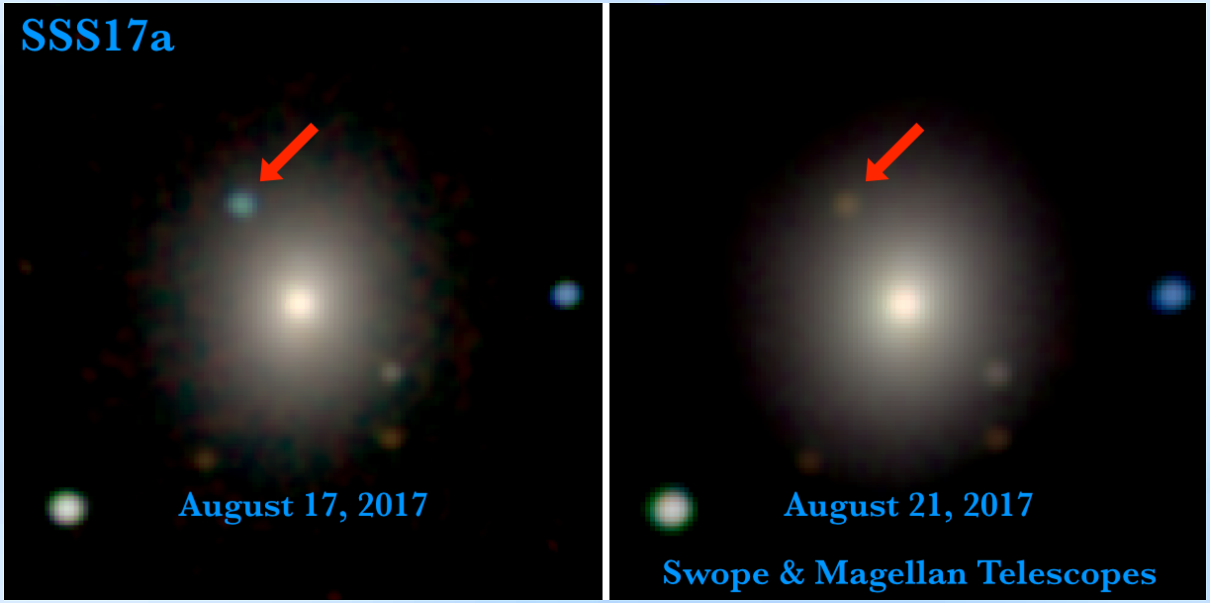

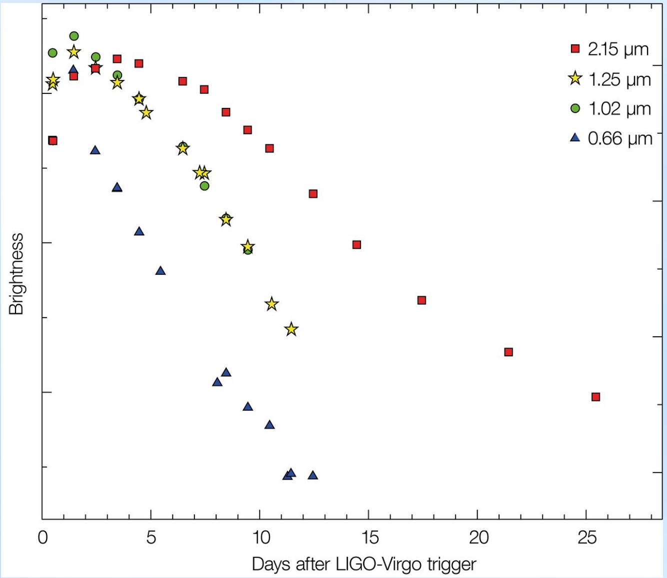

An initially blue signals that fades and turns to red.

Future -
Rapid follow-up of events a necessity.
For example, GRANDMA network.

There might not be a gamma-ray burst, hence need to directly find kilonova in UV-optical-IR

All that glisters is not gold—
Often have you heard that told.

A New Measurement of the Hubble Constant

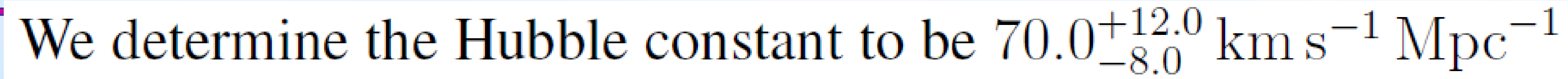
We determine the Hubble constant to be $70.0^{+12.0}_{-8.0}\ \mathrm{km\,s^{-1}\,Mpc^{-1}}$

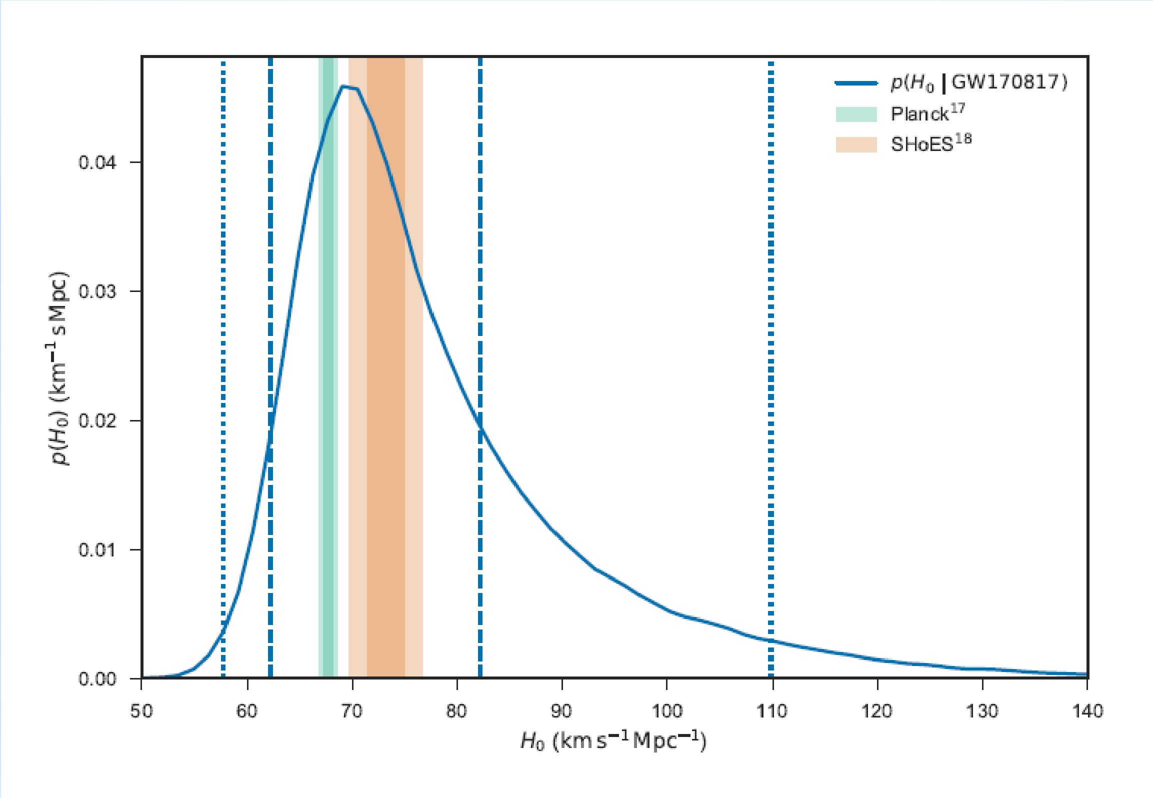

“Our measurement combines the distance to the source inferred purely from the gravitational-wave signal with the recession velocity inferred from measurements of the redshift using electromagnetic data.”

Future: More observations and a better estimate of H_0.

Break tension H_0?

Tidal Effects and Equation of State of Nuclear Material

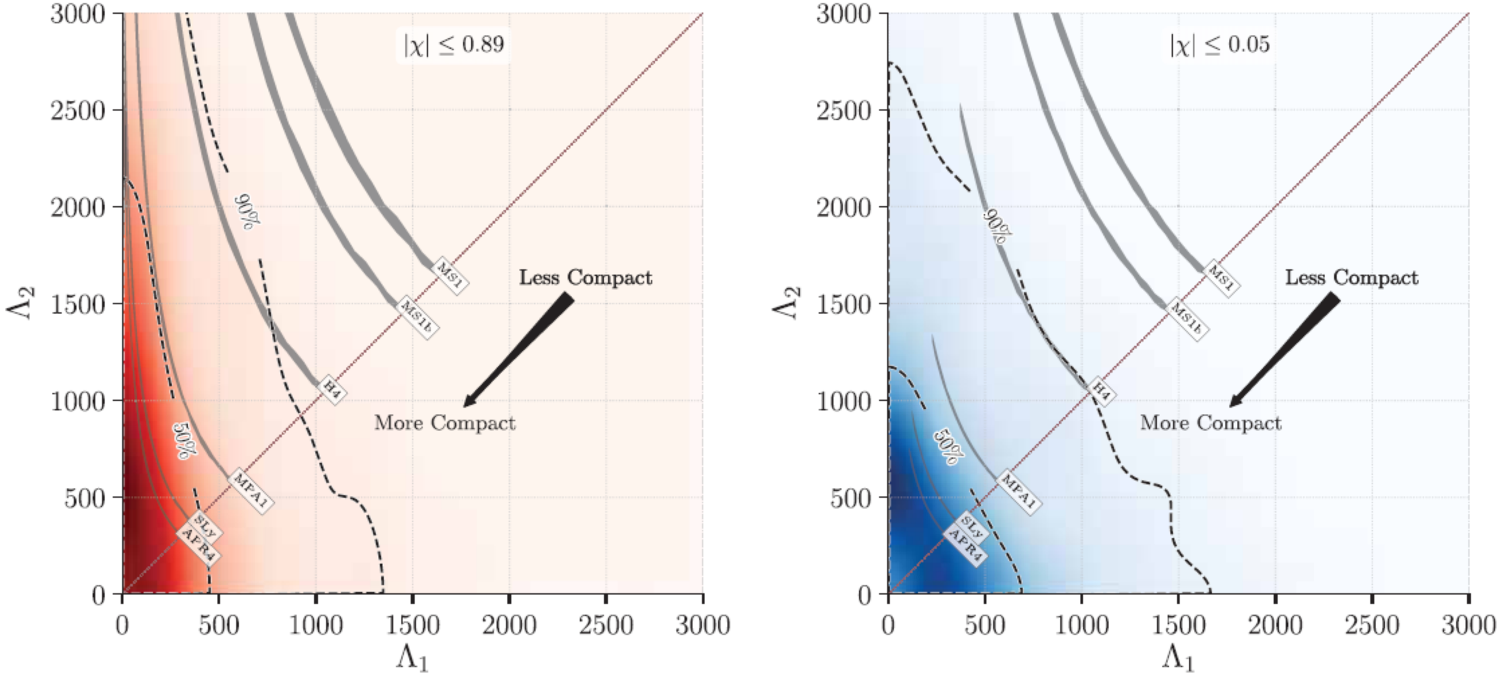

FIG. 5. Probability density for the tidal deformability parameters of the high and low mass components inferred from the detected signals using the post-Newtonian model. Contours enclosing 90% and 50% of the probability density are overlaid (dashed lines). The diagonal dashed line indicates the $\Lambda_1 = \Lambda_2$ boundary. The Λ_1 and Λ_2 parameters characterize the size of the tidally induced mass deformations of each star and are proportional to $k_2(R/m)^5$. Constraints are shown for the high-spin scenario $|\chi| \leq 0.89$ (left panel) and for the low-spin $|\chi| \leq 0.05$ (right panel). As a comparison, we plot predictions for tidal deformability given by a set of representative equations of state [156–160] (shaded filled regions), with labels following [161], all of which support stars of $2.01 M_\odot$. Under the assumption that both components are neutron stars, we apply the function $\Lambda(m)$ prescribed by that equation of state to the 90% most probable region of the component mass posterior distributions shown in Fig. 4. EOS that produce less compact stars, such as MS1 and MS1b, predict Λ values outside our 90% contour.

Future: Important opportunity for nuclear physicists

LIGO-Virgo Measure of Compact Binary Mass Distributions

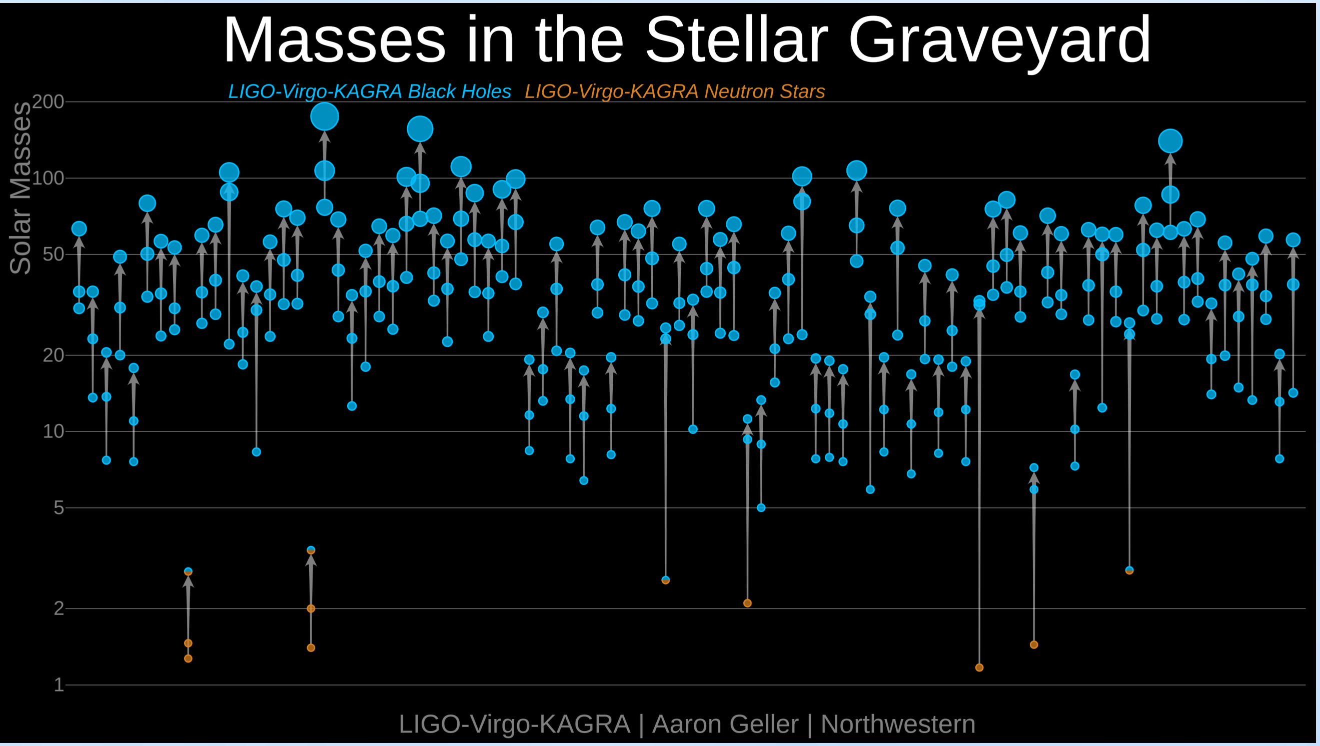

O3 – April 2019 to March 2020. Stopped early due to Covid.

Catalog of 90 events for O1+O2+O3

Culmative catalog

2 binary neutron star mergers

At least 2 NS-BH events

Majority of events are binary black holes

Interesting O3 Events - GW190425

- 2^{nd} binary neutron star observation
- Total Mass ~ 3.4 $M_\odot$
    - M_1 = 1.61 – 2.52 $M_\odot$
    - M_2 = 1.12 – 1.68 $M_\odot$
- Heaviest binary neutron star system
- No EM counterpart observed, 159 Mpc
- GW170817 Total Mass ~ 2.74 $M_\odot$
- Heaviest neutron star known from EM observations (PSR J0740+6620) M ~ 2.05–2.24

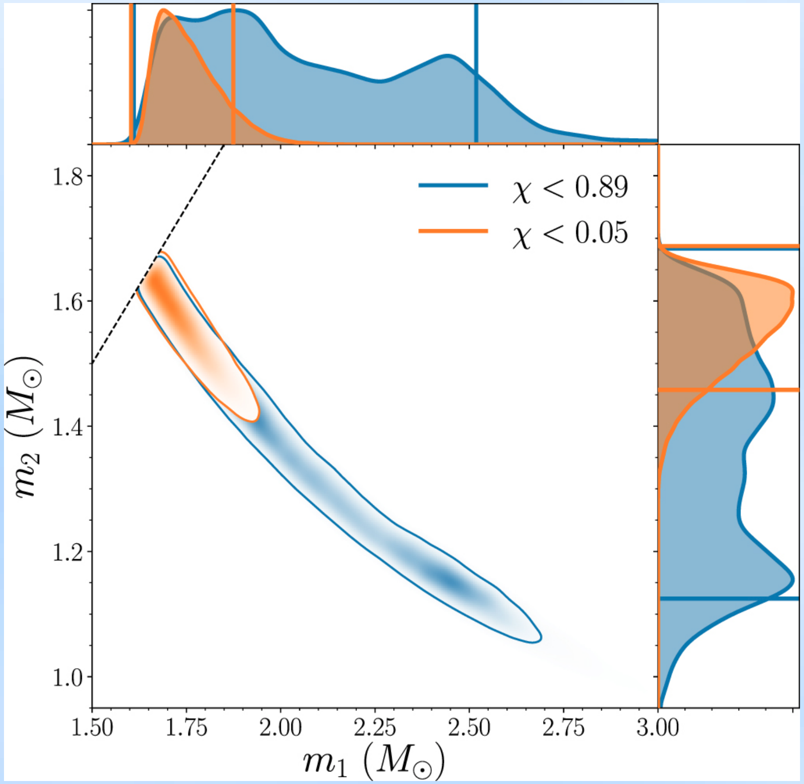

Interesting O3 Events - GW190412

- Unequal mass binary black hole merger
- $M_1 \sim 30\ M_\odot$, $M_2 \sim 8\ M_\odot$
- Asymmetric systems emit gravitational waves with stronger contributions from higher multipoles
- Observe strong evidence for gravitational radiation beyond the leading quadrupolar order in observed signal.

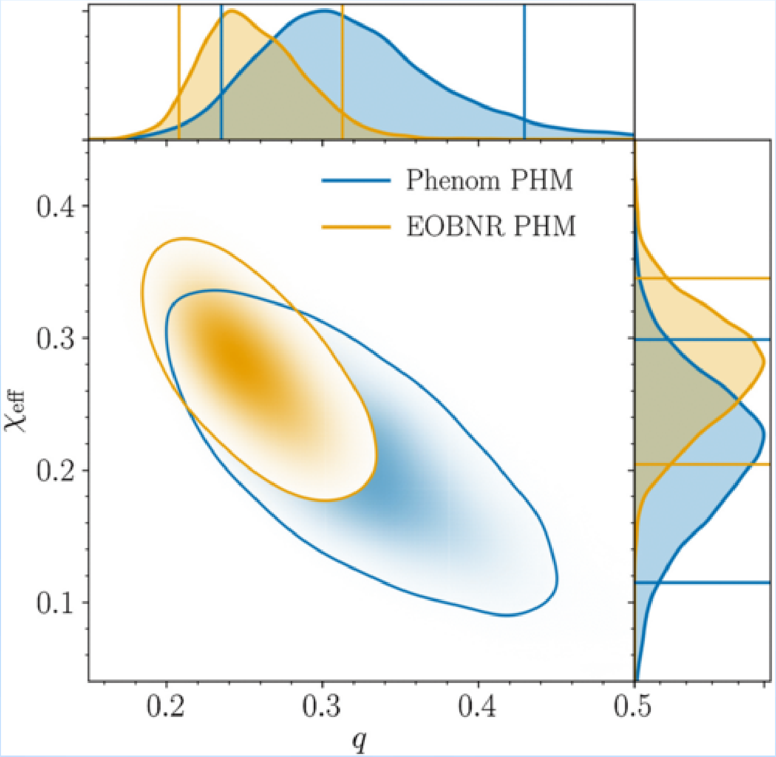

Spin vs. mass ratio, $q = M_2/M_1$

Interesting O3 Events - GW190814

- Another unequal compact binary merger
- $M_1 \sim 23\ M_\odot$, $M_2 \sim 2.50 – 2.67\ M_\odot$
- What is M_2?
  - A very large neutron star?
  - A very small black hole?

  - Above the heaviest known neutron star, MSP J0740+6620
  - Below the typical masses of black holes detected indirectly through EM observations.

  - Mass is compatibles with remnant of a binary neutron star merger

- GW190814 poses a challenge for our understanding of the population of merging compact binaries

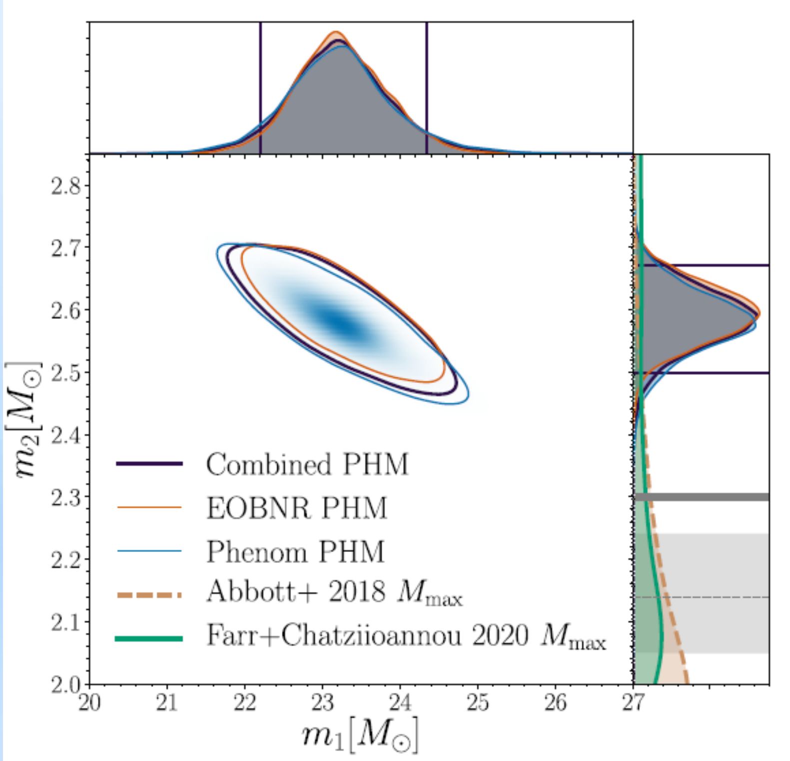

GW190814: “Signal models that exclude higher multipoles or precession do not constrain the secondary mass as well.”

Interesting O3 Events - GW190521

- The GW signal is consistent with a BBH merger source, with total mass of **150 $M_\odot$** .
  - $M_1 \sim 85\ M_\odot$, $M_2 \sim 66\ M_\odot$, $M_{final} \sim 142\ M_\odot$
  - 5.3 Gpc, z ~ 0.82; age of universe was 6.7 Gyr
- System had large spin in orbital plane → precession
- The final merged (remnant) black hole is an **Intermediate Mass Black Hole (IMBH)**.
- The more massive of the two BHs in binary is ~ 85 $M_\odot$, **in the Pair Instability Supernova mass gap**.
- It may itself be the result of a previous BBH merger.

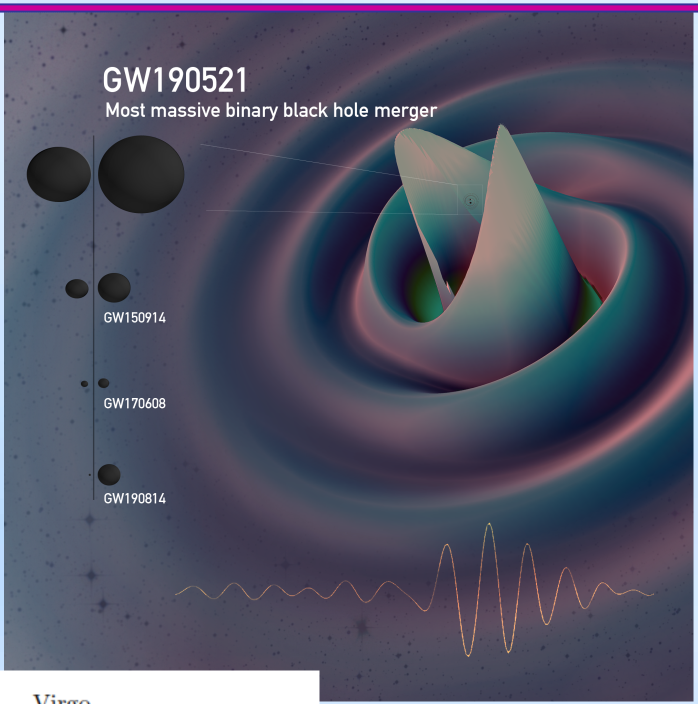

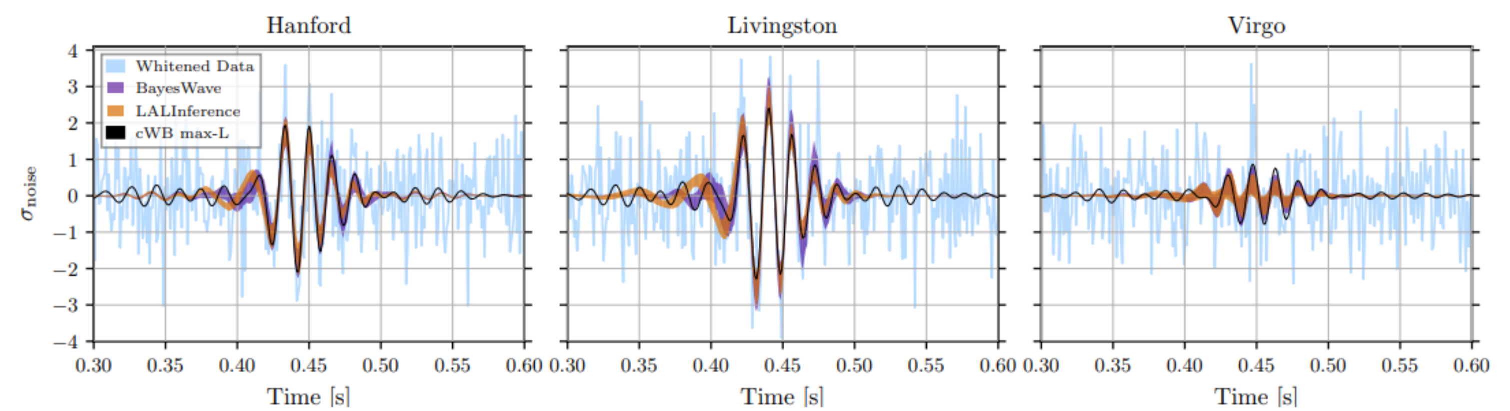

Interesting O3 Events – NS + BH Binaries

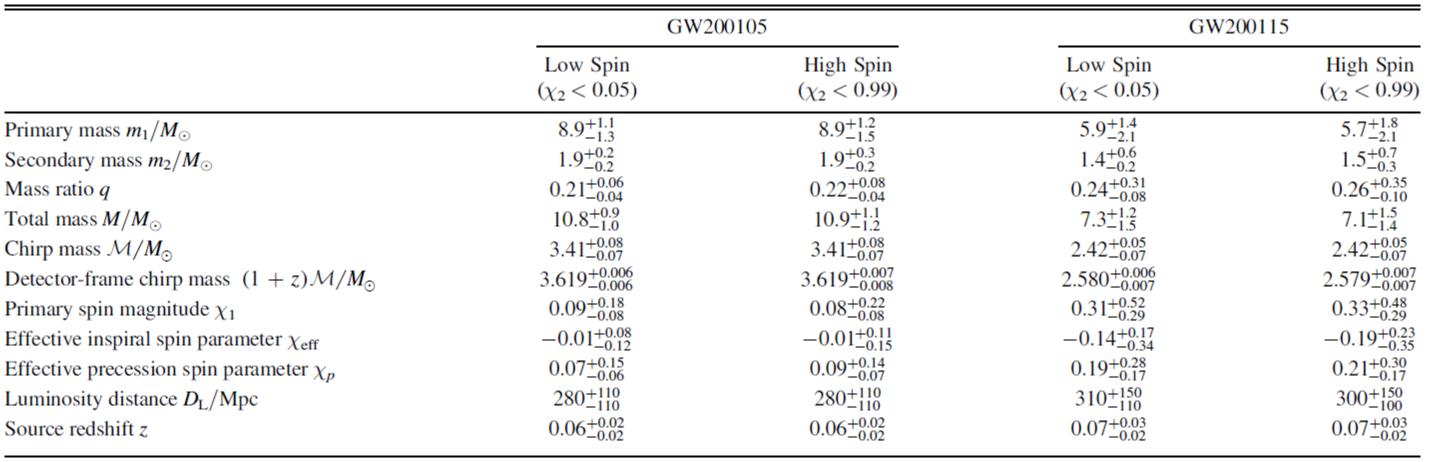

	GW200105		GW200115	
	Low Spin ($\chi_2 < 0.05$)	High Spin ($\chi_2 < 0.99$)	Low Spin ($\chi_2 < 0.05$)	High Spin ($\chi_2 < 0.99$)
Primary mass $m_1/M_\odot$	$8.9^{+1.1}_{-1.3}$	$8.9^{+1.2}_{-1.5}$	$5.9^{+1.4}_{-2.1}$	$5.7^{+1.8}_{-2.1}$
Secondary mass $m_2/M_\odot$	$1.9^{+0.2}_{-0.2}$	$1.9^{+0.3}_{-0.2}$	$1.4^{+0.6}_{-0.2}$	$1.5^{+0.7}_{-0.3}$
Mass ratio q	$0.21^{+0.06}_{-0.04}$	$0.22^{+0.08}_{-0.04}$	$0.24^{+0.31}_{-0.08}$	$0.26^{+0.35}_{-0.10}$
Total mass $M/M_\odot$	$10.8^{+0.9}_{-1.0}$	$10.9^{+1.1}_{-1.2}$	$7.3^{+1.2}_{-1.5}$	$7.1^{+1.5}_{-1.4}$
Chirp mass $\mathcal{M}/M_\odot$	$3.41^{+0.08}_{-0.07}$	$3.41^{+0.08}_{-0.07}$	$2.42^{+0.05}_{-0.07}$	$2.42^{+0.05}_{-0.07}$
Detector-frame chirp mass $(1+z)\mathcal{M}/M_\odot$	$3.619^{+0.006}_{-0.006}$	$3.619^{+0.007}_{-0.008}$	$2.580^{+0.006}_{-0.007}$	$2.579^{+0.007}_{-0.007}$
Primary spin magnitude χ_1	$0.09^{+0.18}_{-0.08}$	$0.08^{+0.22}_{-0.08}$	$0.31^{+0.52}_{-0.29}$	$0.33^{+0.48}_{-0.29}$
Effective inspiral spin parameter $\chi_{\rm eff}$	$-0.01^{+0.08}_{-0.12}$	$-0.01^{+0.11}_{-0.15}$	$-0.14^{+0.17}_{-0.34}$	$-0.19^{+0.23}_{-0.35}$
Effective precession spin parameter χ_p	$0.07^{+0.15}_{-0.06}$	$0.09^{+0.14}_{-0.07}$	$0.19^{+0.28}_{-0.17}$	$0.21^{+0.30}_{-0.17}$
Luminosity distance D_L/Mpc	280^{+110}_{-110}	280^{+110}_{-110}	310^{+150}_{-110}	300^{+150}_{-100}
Source redshift z	$0.06^{+0.02}_{-0.02}$	$0.06^{+0.02}_{-0.02}$	$0.07^{+0.03}_{-0.02}$	$0.07^{+0.03}_{-0.02}$

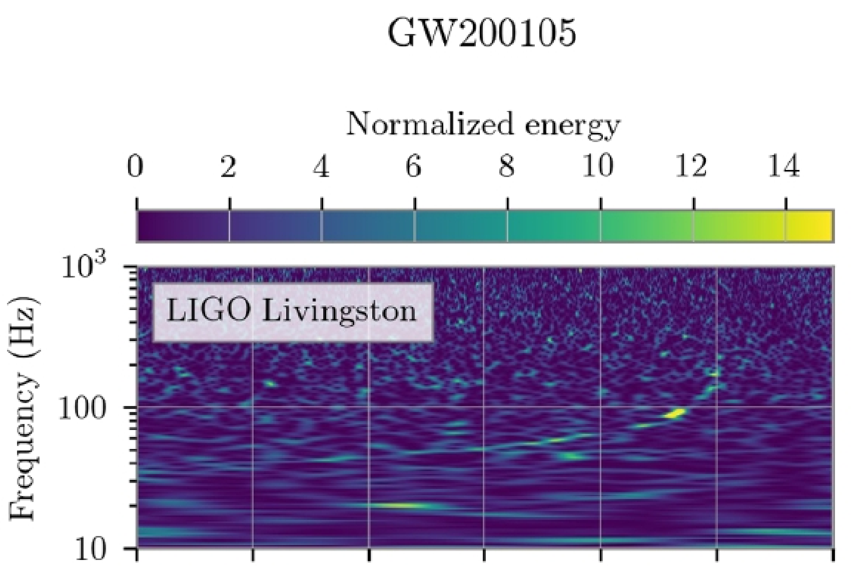

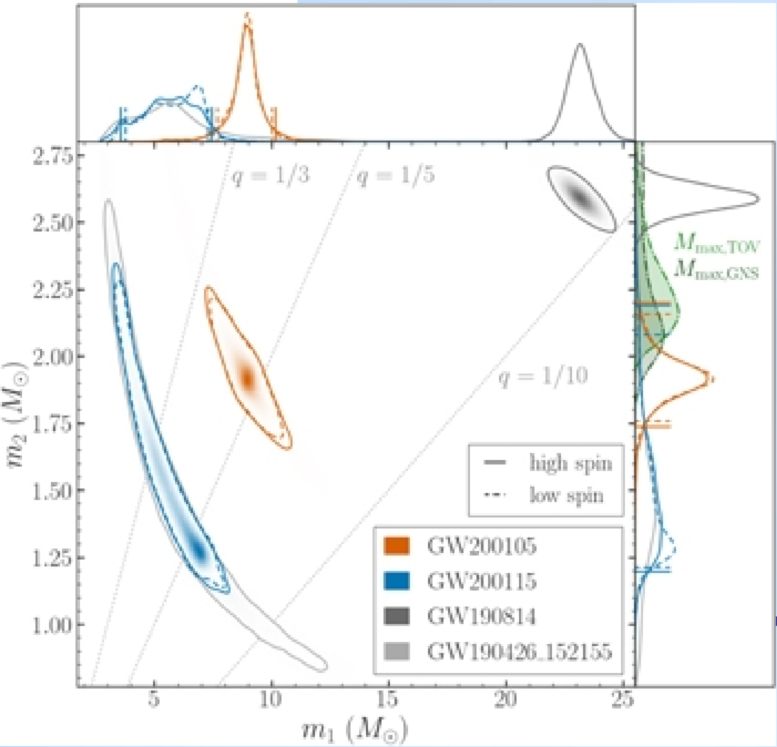

LIGO- Virgo Catalog 3

Some Highlights

- GW191219_163120: NS - BH 31 M⊙ + 1.2 M⊙. NS is one of the least massive ever observed.
- GW200220_061928: Total mass 148 M⊙ (87 M⊙ + 61 M⊙ for each black hole). Final black hole 141 M⊙ → IMBH
- GW191129_134029: 17.5 M⊙ (10.7 M⊙ + 6.7 M⊙). Small!
- GW191109_010717: Negative effective inspiral spin (65 M⊙ + 47 M⊙).

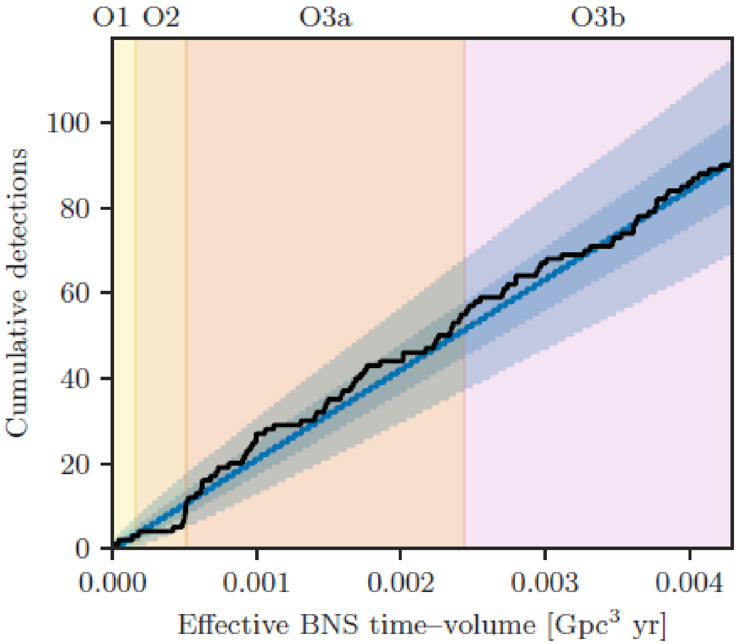

Figure 1. The number of CBC detection candidates with a probability of astrophysical origin $p_{\rm astro} > 0.5$ versus the detector network's effective surveyed time–volume for BNS coalescences [3]. The colored bands indicate the different observing runs. The final data sets for O1, O2, O3a and O3b consist of 49.4 days, 124.4 days, 149.8 days (177.2 days) and 125.5 days (142.0 days) with at least two detectors (one detector) observing, respectively. The cumulative number of probable candidates is indicated by the solid black line, while the blue line, dark blue band and light blue band are the median, 50% confidence interval and 90% confidence interval for a Poisson distribution fit to the number of candidates at the end of O3b.

Stochastic Gravitational-Wave Background

- Upper limit on normalized energy density $\Omega_{GW} < 5.8 \times 10^{-9}$ at 25 Hz
- Approaching level of stochastic background binary produced by compact binary mergers over the history of the universe
- Ultimate goal is to detect a stochastic background from early Universe
    - Astrophysical sources obscure this signal

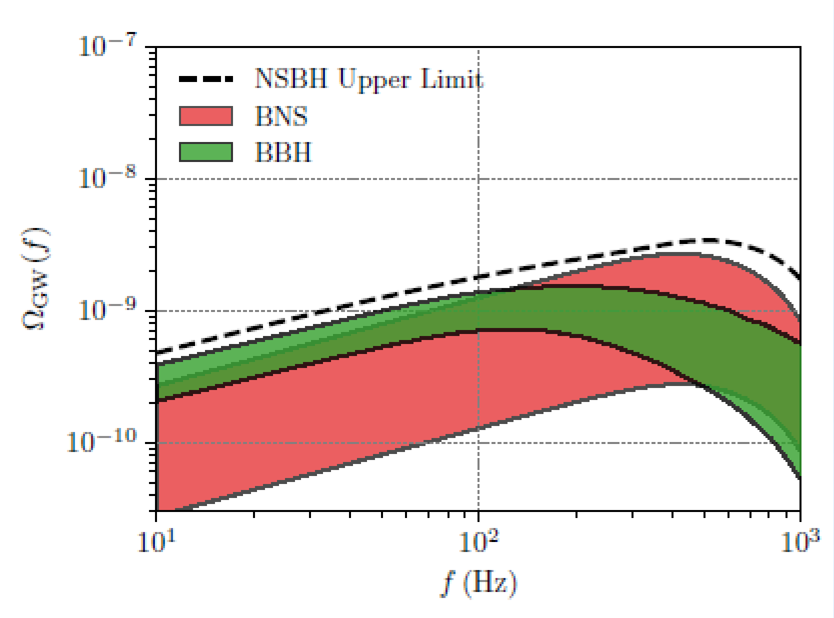

A detector network

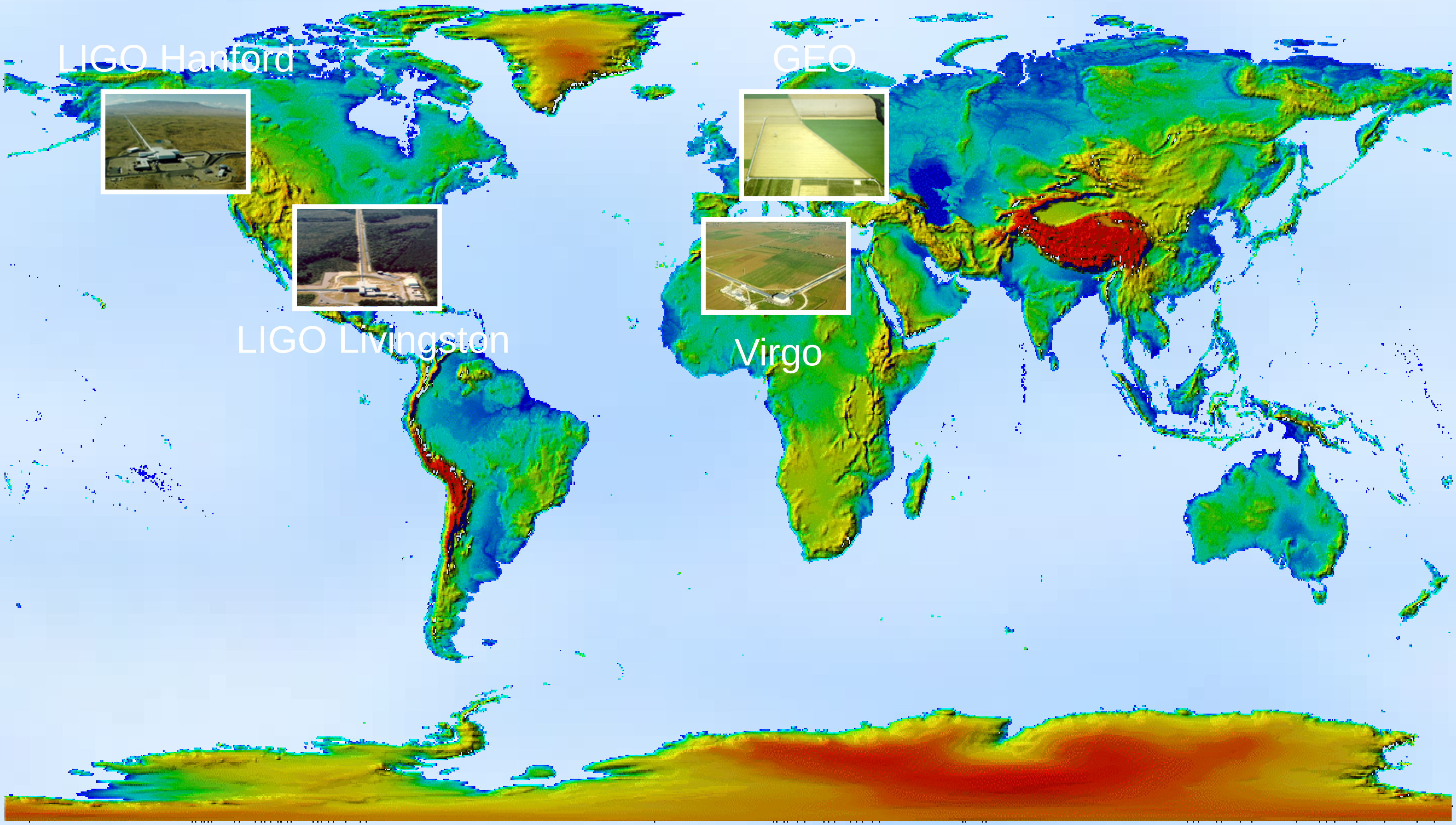

An even better detector network

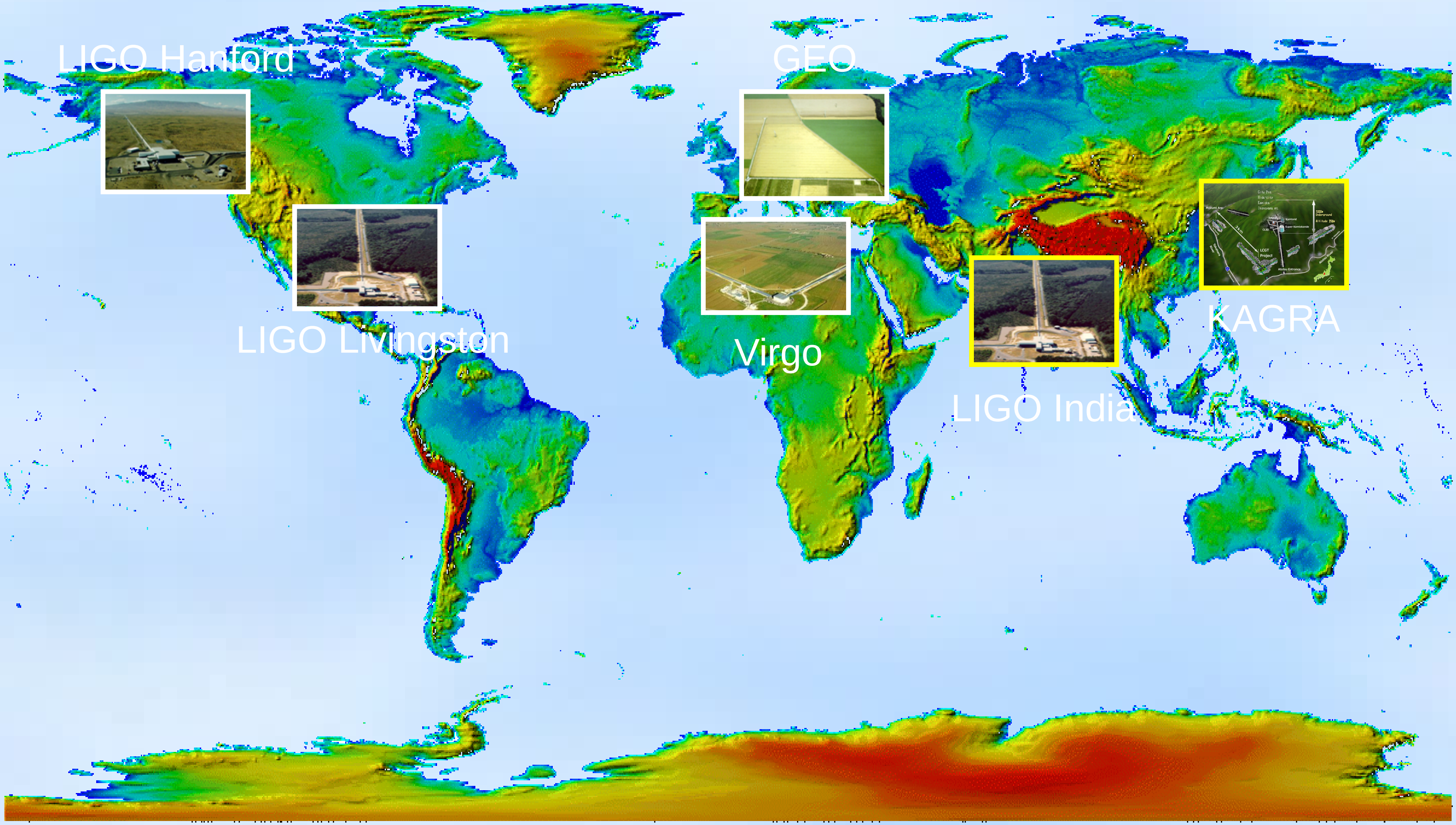

Expected Advanced LIGO-Virgo-KAGRA Sensitivities

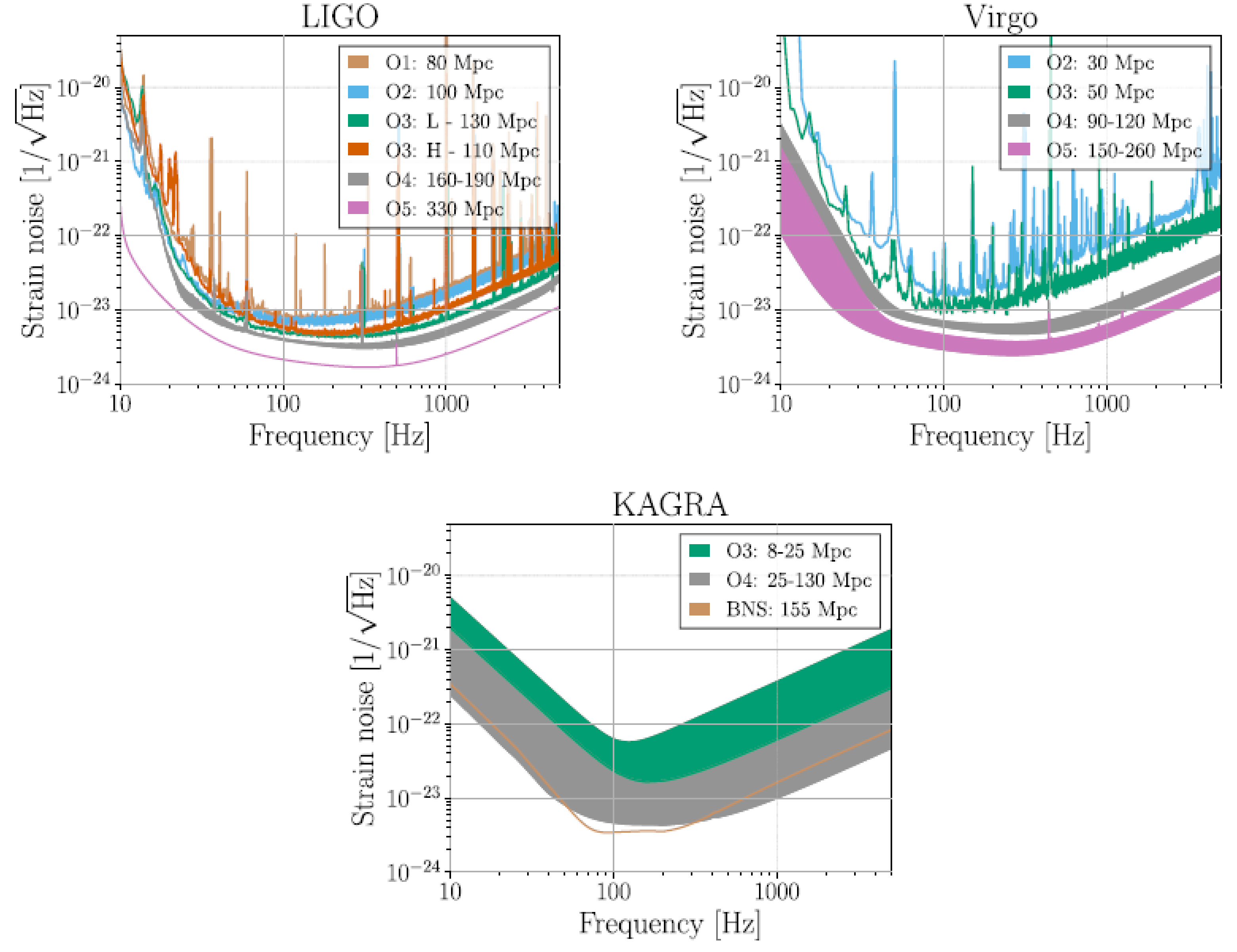

O4, late 2022, LIGO – Virgo - KAGRA

Future Observing Runs

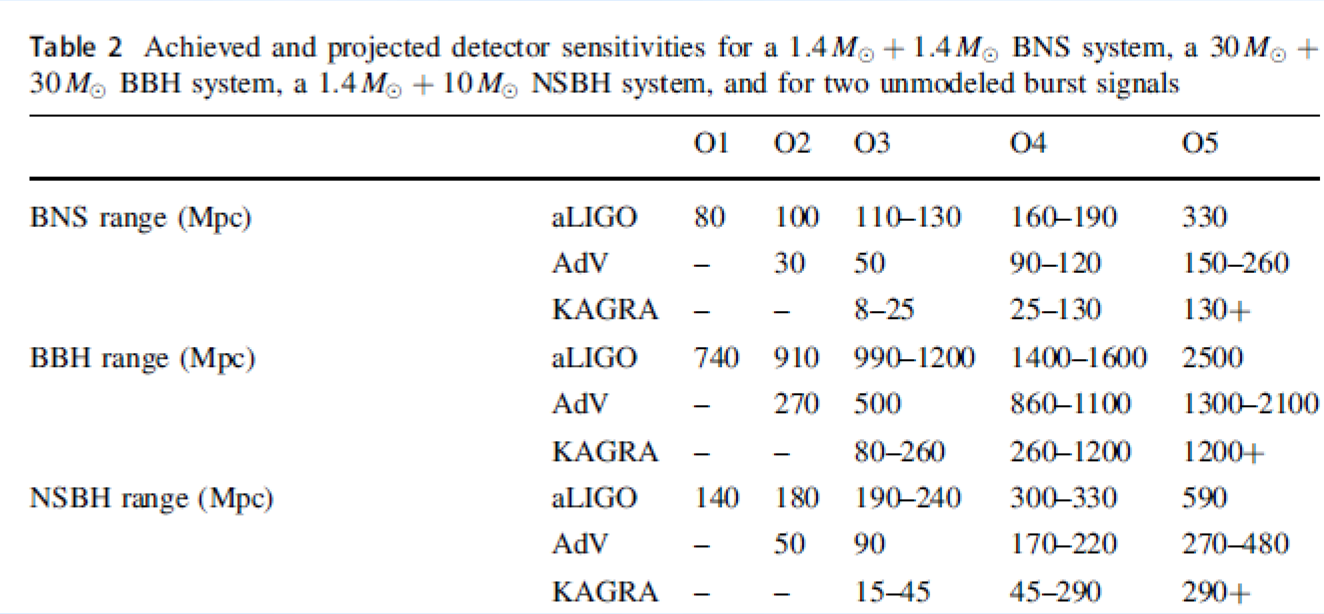

Table 2 Achieved and projected detector sensitivities for a $1.4\,M_\odot + 1.4\,M_\odot$ BNS system, a $30\,M_\odot + 30\,M_\odot$ BBH system, a $1.4\,M_\odot + 10\,M_\odot$ NSBH system, and for two unmodeled burst signals

		O1	O2	O3	O4	O5
BNS range (Mpc)	aLIGO	80	100	110–130	160–190	330
	AdV	–	30	50	90–120	150–260
	KAGRA	–	–	8–25	25–130	130+
BBH range (Mpc)	aLIGO	740	910	990–1200	1400–1600	2500
	AdV	–	270	500	860–1100	1300–2100
	KAGRA	–	–	80–260	260–1200	1200+
NSBH range (Mpc)	aLIGO	140	180	190–240	300–330	590
	AdV	–	50	90	170–220	270–480
	KAGRA	–	–	15–45	45–290	290+

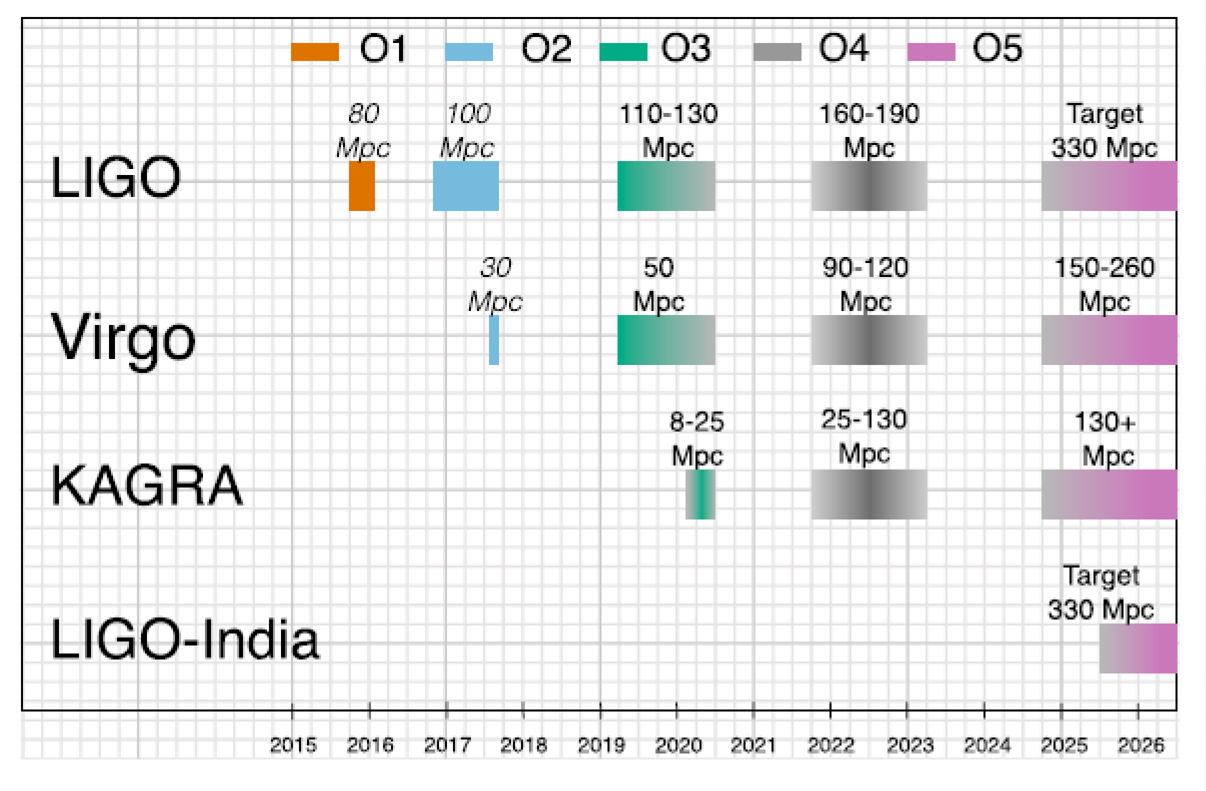

LIGO – Virgo - KAGRA Summary

- Gravitational waves have been observed: black holes and neutron stars
- The universe has more stellar mass black holes than expected
- Gravitational-wave multi-messenger astronomy has started!
- Observing run O3 completed, 90 detections announced for O1 + O2 + O3
- O4 will start in December 2022.
- KAGRA will participate to O4
- LIGO-India will join in ~ 2027
- The future looks bright for ground based detectors

Gravitational Wave Spectrum

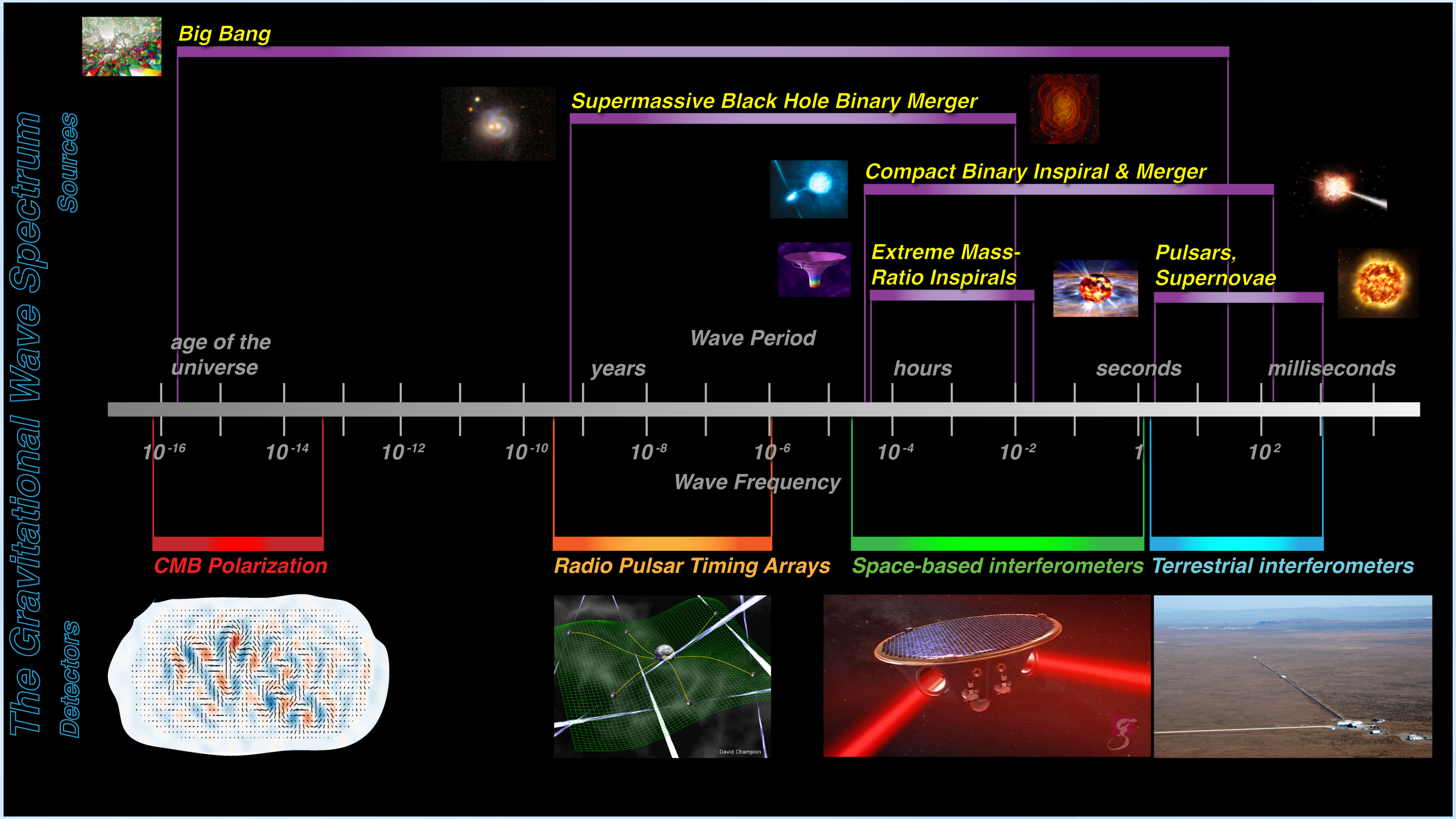

Third Generation Gravitational Wave Detectors

Einstein Telescope

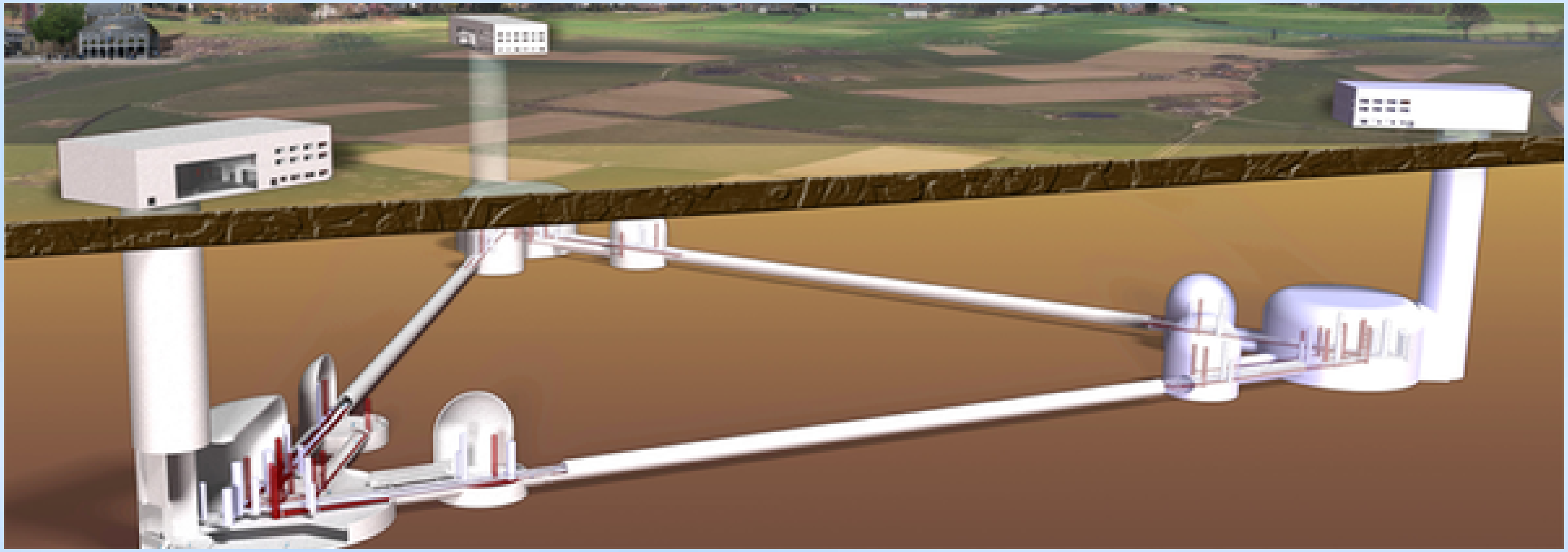

Underground to reduced seismic noise.
10 km arms
Cryogenic mirrors
Lower frequency limit, ~ 1 Hz
10 x better sensitivity than 2nd generation detectors
Farther back in the universe

Noise Sources Limiting the 2G Detectors

- Quantum noise limits most of the frequency range.
- Coating Brownian noise limits in the range from 50 to 100Hz.
- Below ~15Hz we are limited by ‘walls’ made of Suspension Thermal, Gravity Gradient and Seismic noise.
- And then there are the, often not mentioned, ‘technical’ noise sources which trouble the commissioners so much.

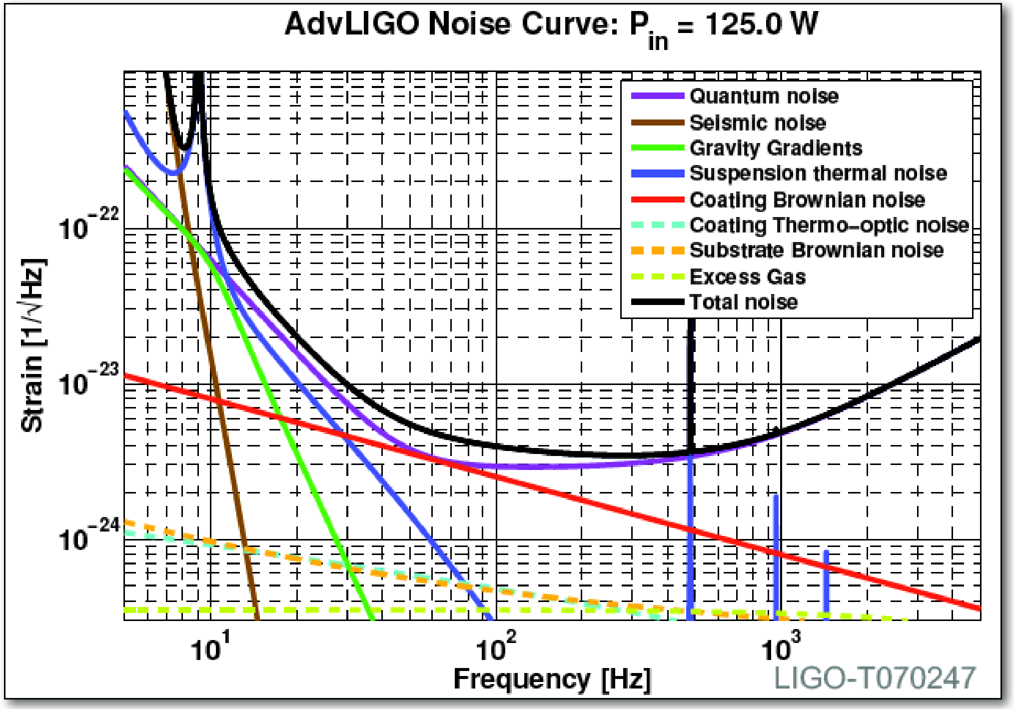

3rd Generation Detectors, To Do List

- Increase arm length, 3km → 10 km: decrease all displacement noises by ~ 3
- Optimizing signal recycling (tuned SR)
- Increase laser power: 125 W to 500 W at IFO input. Reduce shot noise but increase radiation pressure
- Quantum noise suppression: squeezed light
- Increase the beam size → decrease coating Brownian noise
- Cool the test masses: 20 K and decrease Brownian noise
- Longer suspensions: 50 m, 5 stage, corner frequency 0.16 Hz and bring seismic noise wall from 10 Hz down to 1.5 Hz
- Go underground: decrease seismic noise and gravity gradient noise
- Gravity gradient suppression (seismic arrays)
- Heavier mirrors: 42 kg → 120 kg, reduce radiation pressure noise

Einstein Telescope – Very Ambitious Goals

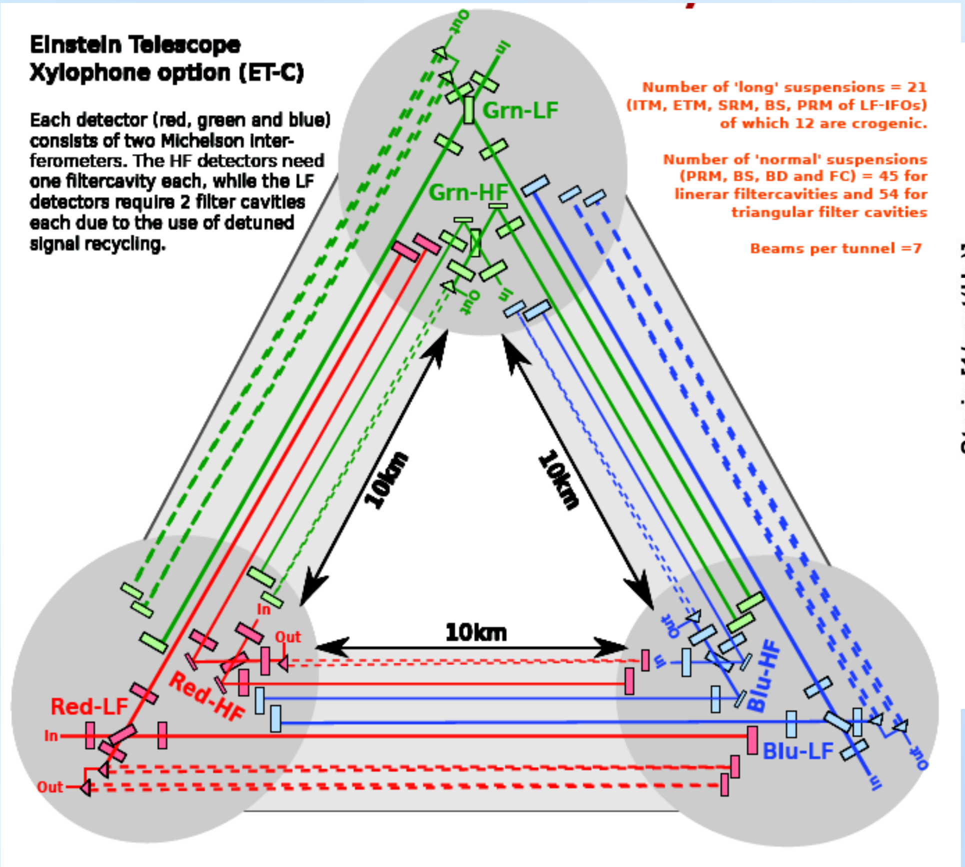

Einstein Telescope Xylophone option (ET-C)

Each detector (red, green and blue) consists of two Michelson interferometers. The HF detectors need one filtercavity each, while the LF detectors require 2 filter cavities each due to the use of detuned signal recycling.

Number of 'long' suspensions = 21 (ITM, ETM, SRM, BS, PRM of LF-IFOs) of which 12 are crogenic.

Number of 'normal' suspensions (PRM, BS, BD and FC) = 45 for linerar filtercavities and 54 for triangular filter cavities

Beams per tunnel =7

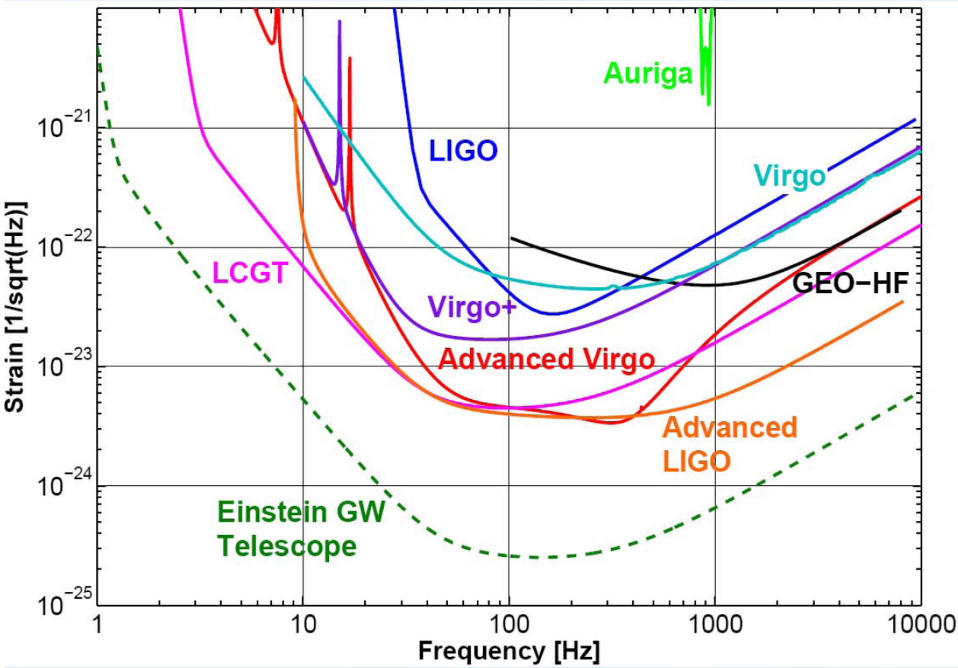

As well, in the US:
LIGO Voyager, 4 km cryogenic
Cosmic Explorer: 40 km interferometer

3G Science

- Advance exploration of extremes of gravity and astrophysics
- Address fundamental questions in physics and astronomy
- Provide insights into most powerful events in the Universe
- Reveal new objects and phenomena
- Try to identify observations that:
  - Will lead to breakthrough science
  - Are uniquely available with gravitational wave observations, possibly in conjunction with EM observations
  - Can only be achieved with the sensitivity of 3rd generation detectors such as Einstein Telescope

Laser Interferometer Space Antenna - LISA

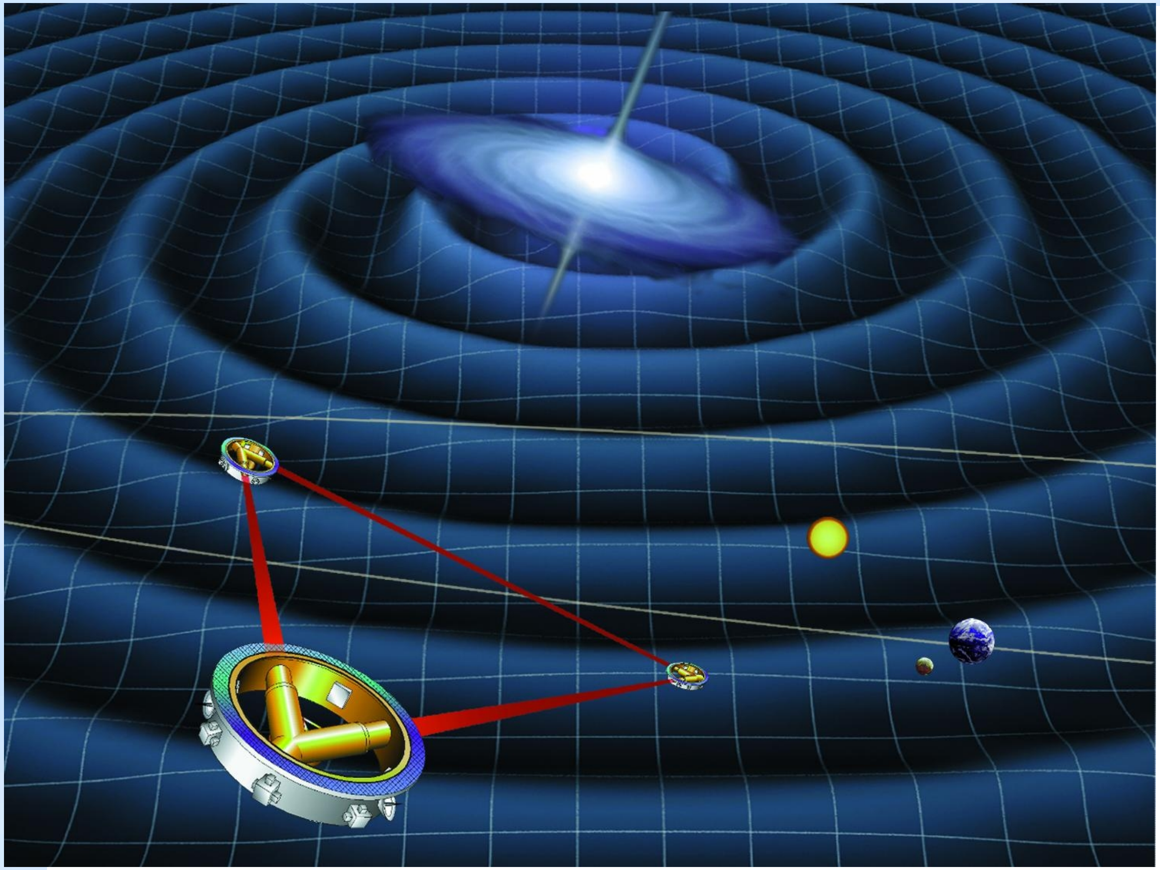

ESA – All Systems GO!

Planned launch 2034

NASA as a junior partner

LIGO-Virgo GW events and Lisa Pathfinder success have helped significantly

Tremendous activity at Present

Major French involvement

Present plan: 3 Interferometers
2.5 x 10^6 km arm lengths

LISA Pathfinder – Demonstrating LISA Technology

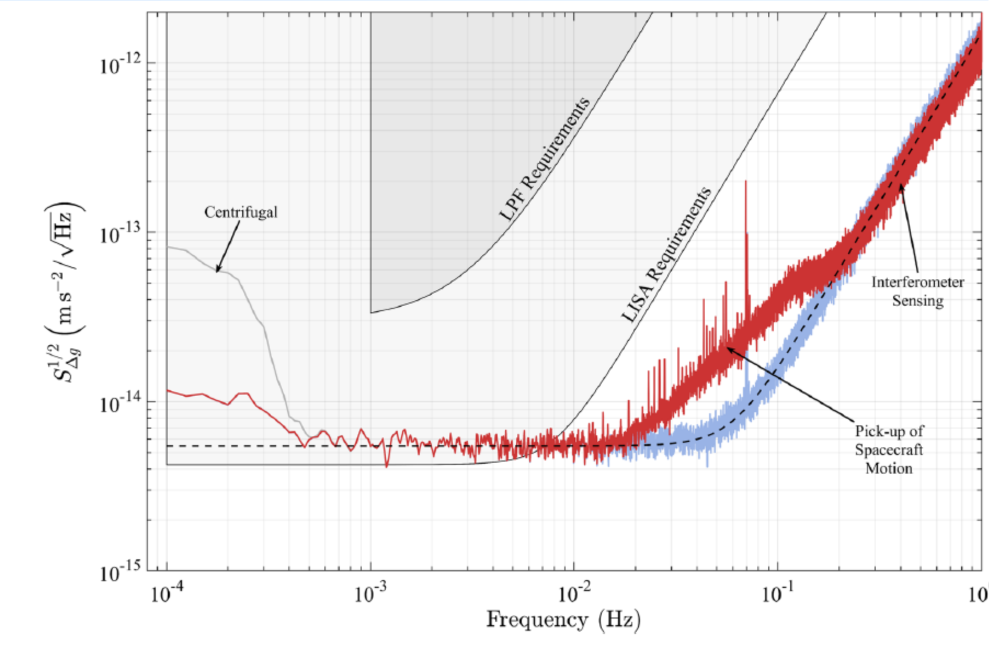

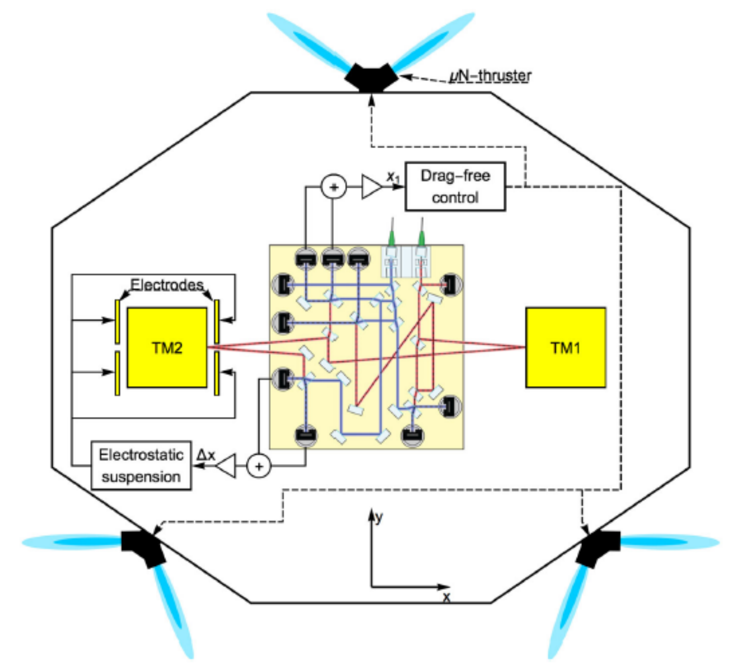

LISA Pathfinder worked! Exceeded requirements. Still, operation was not perfect, and there is lots of experimental work to do before LISA.

A set of cold gas micro-newton thrusters to ensure the spacecraft follows TM1. A second control loop forces TM2 to stay at a fixed distance from TM1 and thus centered in its own electrode housing.

PRL **116**, 231101 (2016)

LISA Physics

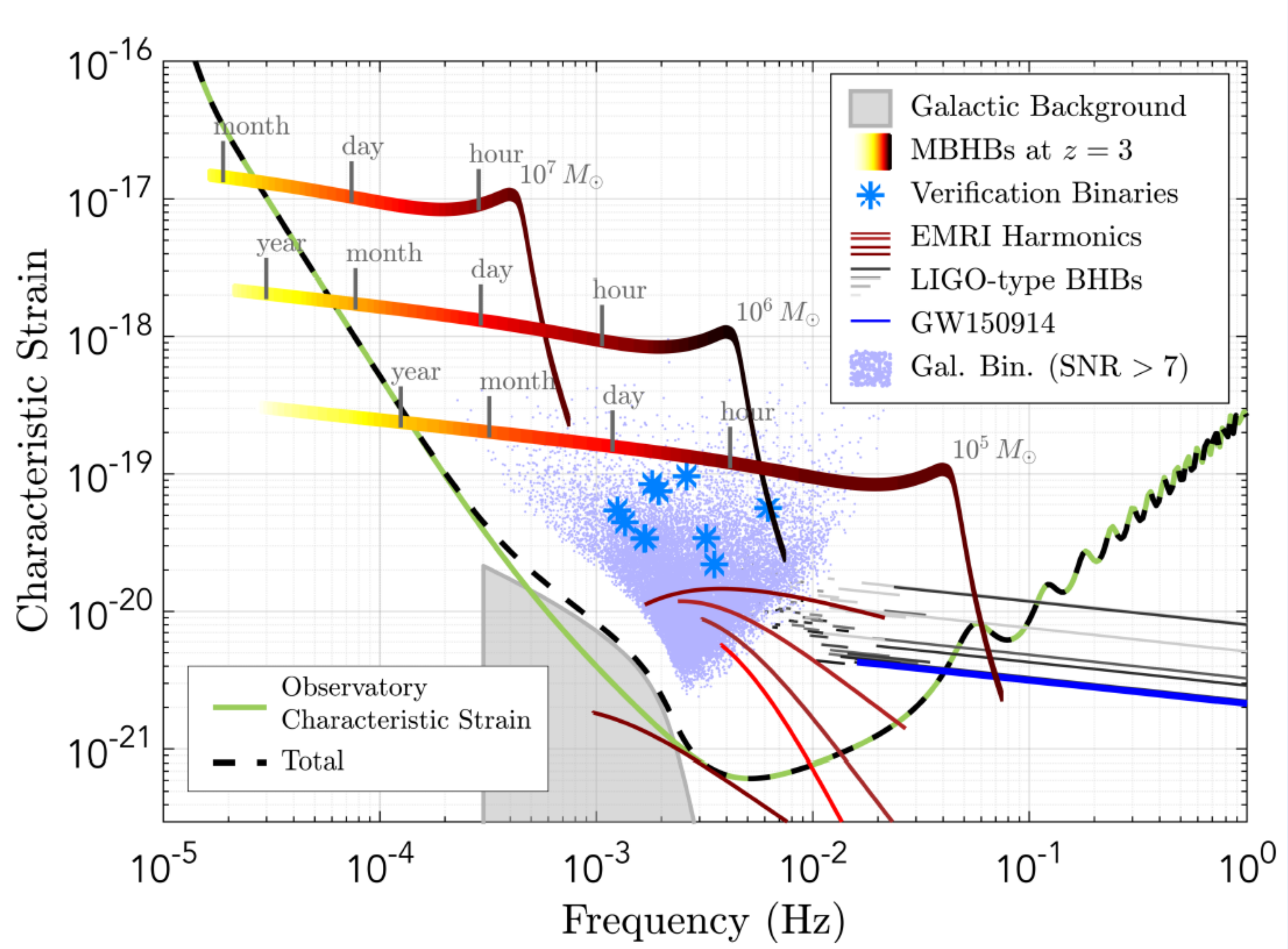

1702.00786

Characteristic strain amplitude versus frequency (arm length 2.5 x 10^6 km, 1-yr observations).

IMBH: Bridge from Stellar Mass to SMBH

- LIGO-Virgo, BBH systens with 100s of solar mass
- Einstein Telescope and Cosmic Explorer, BBH systens with 1000s of solar mass
- LISA, BBH systens with millions of solar mass
- A tremendous opportunity to measure the BBH systems from stellar mass to SMBH
- This can only be done with gravitational wave observations!

Pulsar Timing

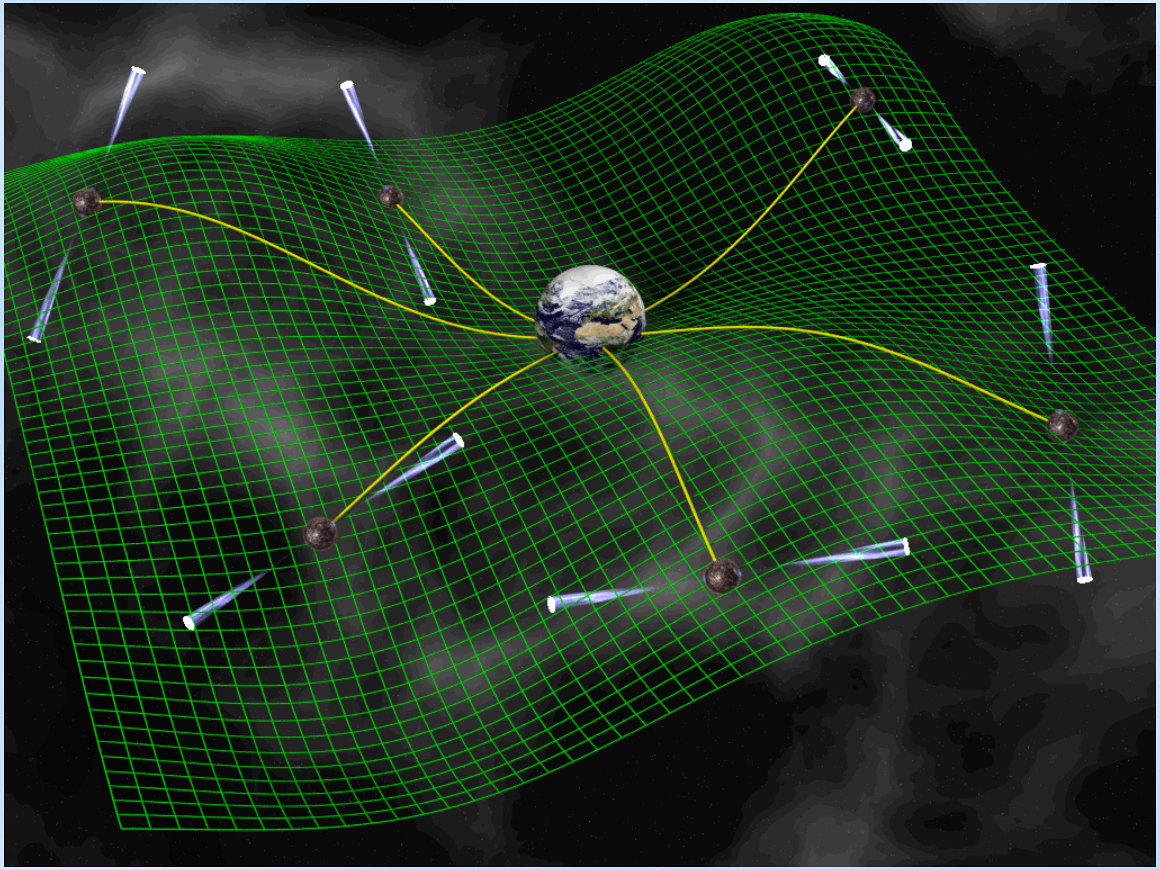

arXiv:1211.4590

Distant pulsars send regular radio pulses – highly accurate clocks.
A passing gravitational wave would change the arrival time of the pulse.

Numerous collaborations around the world. Interesting upper limits and likely detections in the near future.

NANOGrave 12.5 Data Set – A Hint At ASignal?

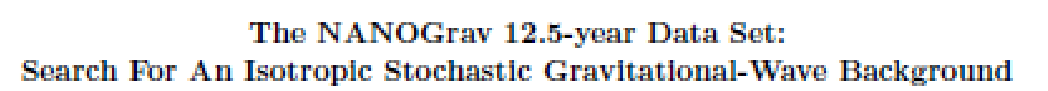

The NANOGrav 12.5-year Data Set:
Search For An Isotropic Stochastic Gravitational-Wave Background

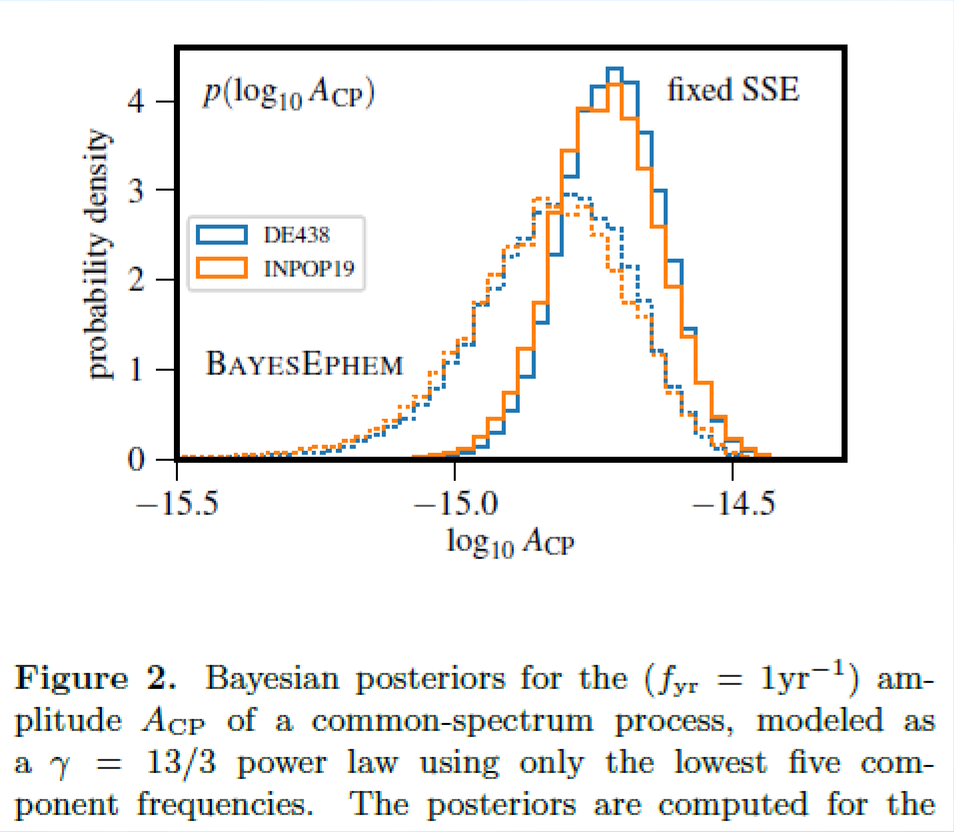

Figure 2. Bayesian posteriors for the ($f_{\mathrm{yr}} = 1\mathrm{yr}^{-1}$) amplitude A_{CP} of a common-spectrum process, modeled as a $\gamma = 13/3$ power law using only the lowest five component frequencies. The posteriors are computed for the

First hint of a signal?

Some bias or “red noise”?

Arxiv is hot with theories: SMBHs, primordial BHs, cosmic strings, …

The coming years of pulsar timing observations could see a confirmed observation.

“Our analysis finds strong evidence of a stochastic process, modeled as a power-law, with common amplitude and spectral slope across pulsars.”

arXiv:2009.04496

Polarization Map of the Cosmic Microwave Background

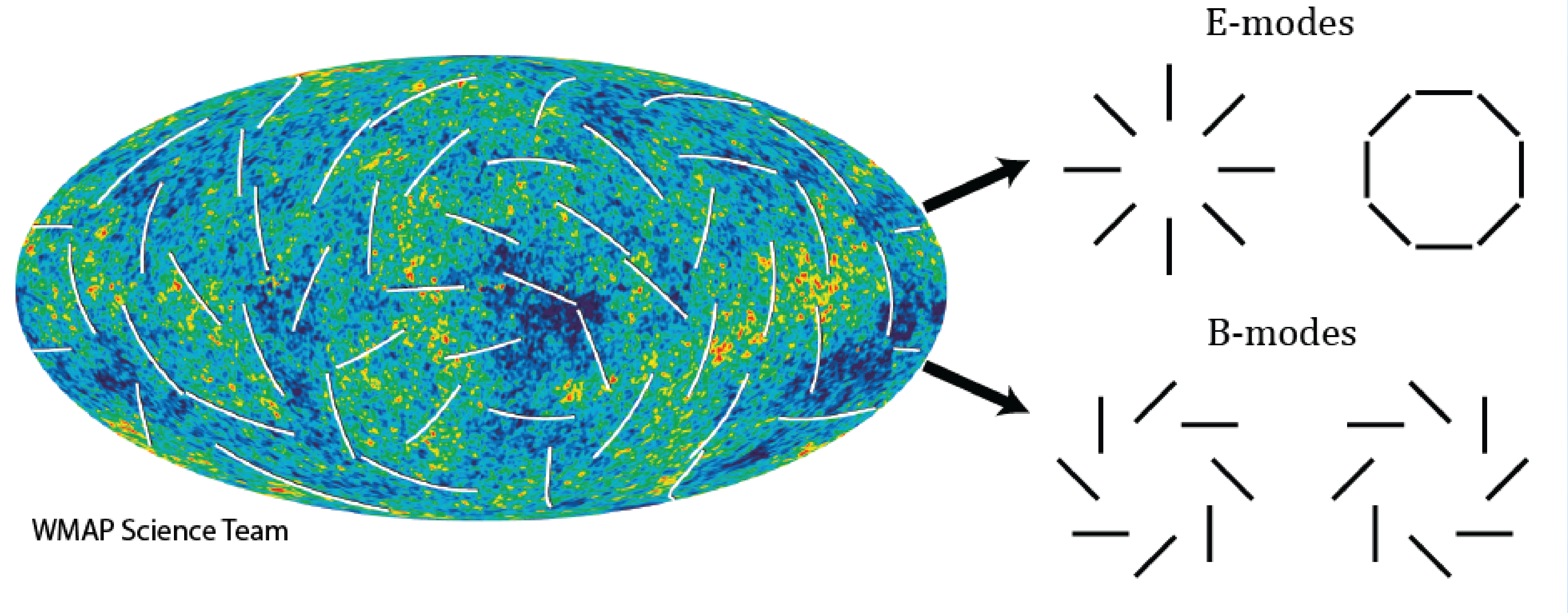

The CMB anisotropy polarization map may be decomposed into curl-free even-parity E-modes and divergence-free odd-parity B-modes.

Gravitational waves in the early universe impart a “curl” on CMB polarization.
ArXiv:1407.2584

BICEP2, KECK Array, Planck, Atacama

Conclusion on Gravitational Waves

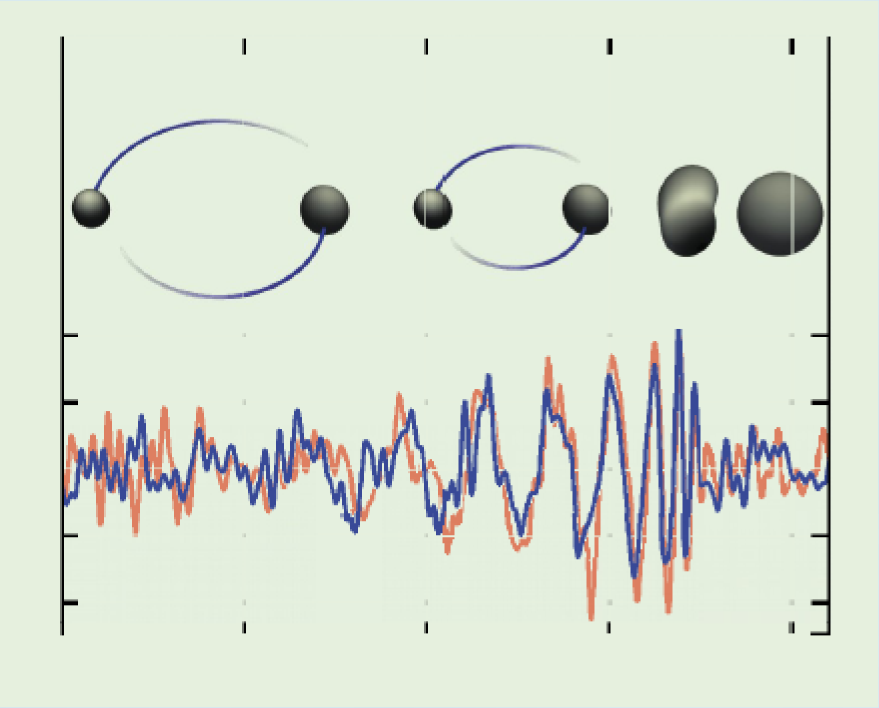

A new window on the universe has opened.

We are just beginning!